A FREQUENCY EVALUATION OF A VIRTUAL REALITY SENSORY INTERACTION BALANCE TEST

Marcel Tesolin

A THESIS SUBMITTED TO THE FACULTY OF GRADUATE STUDIES IN PARTIAL FULFILLMENT OF THE REQUIREMENTS FOR THE DEGREE OF

MASTER OF SCIENCE

GRADUATE PROGRAM IN KINESIOLOGY AND HEALTH SCIENCE

YORK UNIVERSITY

TORONTO, ONTARIO

July 2026

© Marcel Tesolin, 2026

Abstract

Balance is maintained through the integration and weighting of sensory information based on its reliability to allow the nervous system to modulate motor output. The Frequency-Specific Sensory Contribution Framework (FSCF) proposes that distinct frequency bands are related to the visual, vestibular, cerebellar, and proprioceptive contributions to balance. This work aimed to critically examine the FSCF across kinetic and kinematic measures during sensory manipulations. Thirty-two participants performed a Virtual Reality Sensory Interaction Balance Test involving eight different sensory conditions. Results indicate that the FSCF did not fully capture the frequency-specific sensory contributions to balance across measures. Specifically, visual and somatosensory systems contributed to frequencies beyond the FSCF's hypothesized frequency bands, suggesting that the FSCF may be an oversimplification of the complexities of upright stance behaviour. This work proposes a frequency threshold, rather than distinct categories, to more accurately and robustly characterize complex sensory contributions to balance during sensory manipulation.

Acknowledgements

I would like to first thank the guidance of my two supervisors, Dr. Taylor Cleworth and Dr. William Gage, whose support over the past two years made this thesis possible. The mentorship you have both provided me has profoundly impacted this work and laid the foundation for my development as a scientist. Thank you both for your patience and belief in me. The lessons and experience you have both provided me will be carried out in my future work regardless of the field or discipline.

I would also like to thank my supervisory committee, Dr. George Mochizuki and Dr. Veronika Jamnik. Thank you, Dr. Mochizuki, for your guidance and advice during the process of this project and thank you to Dr. Jamnik for providing my first experience in a research setting. Participating in your research lab during my third year of undergraduate degree sparked my curiosity to pursue my Master's degree.

I am very appreciative of all the members of both of my labs, as well as colleagues in the biomechanics section of the Sherman Health Science Research Centre. I would especially like to thank Maureen, Philip, Sara, and Nora for their assistance during data collection and advice throughout the process of this project.

Lastly, and certainly not least, I would like to acknowledge my family, who have provided me with unwavering support throughout my academic journey. Thank you for always believing in me no matter what endeavour I attempt; I could not have done it without you.

Table of Contents

Abstract ..... ***ii***

Acknowledgements ..... ***iii***

Table of Contents ..... ***iv***

List of Tables ..... ***vi***

List of Figures ..... ***vii***

List of Abbreviations ..... ***xi***

Chapter 1: Introduction ***1***

1.1 Maintenance of Upright Stance **2**

1.2 Balance Tests & Tools for Balance Assessment **2**

1.3 Sensory Contributions to Upright Stance **5**

1.3.1 The Role of the Visual System on the Control of Upright Stance *5*

1.3.2 The Role of the Vestibular System on the Control of Upright Stance *6*

1.3.3 The Role of the Somatosensory System on the Control of Upright Stance *8*

1.4 Sensory Integration & Reweighting **9**

1.5 Frequency-Specific Sensory Contribution Framework **11**

1.6 Current Research Gap & Significance **12**

1.7 Purpose **14**

1.8 Research Question & Hypothesis **15**

Chapter 2: Methods ***17***

2.1 Participants **17**

2.2 Procedure **17**

2.3 Experimental Conditions **19**

2.4 Measurements **21**

2.5 Data Analysis **22**

2.6 Statistical Analysis **23**

Chapter 3: Results ***25***

3.1 Participant Demographics **25**

3.2 Summary Results Table **26**

3.3 Total Band Power **27**

3.4 Relative Frequency Composition **32**

3.4.1 Kinetics *32*

3.4.2 Kinematics *38*

3.4.3 EMG *45*

Chapter 4: Discussion *52*
4.1 Total Band Power **54**
4.1.1 Kinetics *54*
4.1.2 Kinematics *55*
4.1.3 Electromyography *56*
4.1.4 Total Band Power Summary *57*
4.2 Composition of the Frequency Bands **59**
4.2.1 Ultra-Low Frequency Band *59*
4.2.2 Low Frequency Band *62*
4.2.3 Medium Frequency Band *64*
4.2.4 High Frequency Band *67*
4.3 Limitations & Future Work **69**
Chapter 5: Conclusions *71*
5.1 A Proposed Framework: Low & High Frequency Control **71**
5.1.2 Low Frequency Domain *72*
5.1.3 High Frequency Domain *73*
References ***75***
Appendices ***89***
Appendix A: AP COP FSCF Predictions vs Actual Results per condition **89**
Appendix B: AP COM FSCF Predictions vs Actual Results per condition **91**
Appendix C: Low & High Frequency Control Figures ~ AP COP **93**

List of Tables

Table 1: A list of the conditions with their corresponding sensory manipulation in the VR-SIBT. 19

Table 2: Participant demographics. 25

Table 3: Results Summary of the AP COP, AP COM, and Right Soleus 26

List of Figures

Figure 1: Frequency band of the sensory systems. Reproduced from Lin et al. (2019), under the Creative Commons Attribution 4.0 International Licence. No changes were made. 11

Figure 2: Experimental set-up with firm (left) & foam (right) surfaces. (EMG sensors for the left TA and right soleus are displayed. Tape markings are not displayed) 19

Figure 3: *Participants' view inside the HMD of the realistic art gallery scene.* 20

Figure 4: Total Band Power for AP COP. Solid bars are firm surface conditions. Hatched bars are foam surface conditions. Colours represent visual conditions as indicated in the legend. Standard error bars are displayed. Significance is indicated between sensory conditions. (*p<0.005, **p<0.001). 28

Figure 5: Total Band Power for AP COM. Solid bars are firm surface conditions. Hatched bars are foam surface conditions. Colours represent visual conditions as indicated in the legend. Standard error bars are displayed. Significance is indicated between sensory conditions. (*p<0.005, **p<0.001). 30

Figure 6: Total Band Power of the right soleus. (Left) Displays the main effect of surface. Grey filled bar represents collapsed firm conditions and the hatched bar represents collapsed foam conditions. (Right) Displays the main effect of vision. Colours represent collapsed visual conditions as indicated in the legend. Standard error bars are displayed for both. Significance is indicated between sensory conditions. (*p<0.005, **p<0.001). 31

Figure 7: Relative frequency composition of AP COP for the ultra-low frequency band (0-0.1Hz). (Left) Displays the main effect of surface. Grey filled bar represents collapsed firm conditions and the hatched bar represents collapsed foam conditions. (Right) Displays the main effect of vision. Colours represent collapsed visual conditions as indicated in the legend. Standard error bars are displayed. Significance is indicated between sensory conditions. (*p<0.005, **p<0.001). 33

Figure 8: Relative frequency composition of AP COP for the low frequency band (0.1-0.5Hz). (Left) Displays the main effect of surface. Grey filled bar represents collapsed firm conditions and the hatched bar represents collapsed foam conditions. (Right) Displays the main effect of vision. Colours represent collapsed visual conditions as indicated in the legend. Standard error bars are displayed. Significance is indicated between sensory conditions. (*p<0.005, **p<0.001). 34

Figure 9: Relative frequency composition of AP COP for the medium frequency band (0.5-1Hz). Solid bars are firm surface conditions. Hatched bars are foam surface conditions. Colours represent visual conditions as indicated in the legend. Standard error bars are displayed. Significance is indicated between sensory conditions. (*p<0.005, **p<0.001). 36

Figure 10: Relative frequency composition of AP COM for the high frequency band (1-5Hz). Solid bars are firm surface conditions. Hatched bars are foam surface conditions. Colours represent visual conditions as indicated in the legend. Standard error bars are displayed. Significance is indicated between sensory conditions. (*p<0.005, **p<0.001). 38

Figure 11: Relative frequency composition of AP COM for the ultra-low frequency band (0-0.1Hz). (Left) Displays the main effect of surface. Grey filled bar represents collapsed firm conditions and the hatched bar represents collapsed foam conditions. (Right) Displays the main effect of vision. Colours represent collapsed visual conditions as indicated in the legend. Standard error bars are displayed. Significance is indicated between sensory conditions. (*p<0.005, **p<0.001). 39

Figure 12: Relative frequency composition of AP COM for the low frequency band (0.1-0.5Hz). (Left) Displays the main effect of surface. Grey filled bar represents collapsed firm conditions and the hatched bar represents collapsed foam conditions. (Right) Displays the main effect of vision. Colours represent collapsed visual conditions as indicated in the legend. Standard error bars are displayed. Significance is indicated between sensory conditions. (*p<0.005, **p<0.001). 41

Figure 13: Relative frequency composition of AP COM for the medium frequency band (0.5-1Hz). Solid bars are firm surface conditions. Hatched bars are foam surface conditions. Colours represent visual conditions as indicated in the legend. Standard error bars are displayed. Significance is indicated between sensory conditions. (*p<0.005, **p<0.001). 43

Figure 14: Relative frequency composition of AP COM for the high frequency band (1-5Hz). Solid bars are firm surface conditions. Hatched bars are foam surface conditions. Colours represent visual conditions as indicated in the legend. Standard error bars are displayed. Significance is indicated between sensory conditions. (*p<0.005, **p<0.001). 45

Figure 15: Relative frequency composition of the Right Soleus for the ultra-low frequency band (0-0.1Hz). The solid bar represents the firm surface conditions, and the hatched bar represents the foam surface conditions. Significance is indicated between sensory conditions. (*p<0.005, **p<0.001). 46

Figure 16: Relative frequency composition of the Right Soleus for the low frequency band (0.1-0.5Hz). Solid bars are firm surface conditions. Hatched bars are foam surface conditions. Colours represent visual conditions as indicated in the legend. Standard error bars are displayed. Significance is indicated between sensory conditions. (*p<0.005, **p<0.001). 48

Figure 17: Relative frequency composition of the right soleus for the medium frequency band (0.5-1Hz). (Left) Displays the main effect of surface. Grey filled bar represents collapsed firm conditions and the hatched bar represents collapsed foam conditions. (Right) Displays the main effect of vision. Colours represent collapsed visual conditions as indicated in the legend. Standard error bars are displayed. Significance is indicated between sensory conditions. (*p<0.005, **p<0.001). 49

Figure 18: Relative frequency composition of the right soleus for the high frequency band (1-5Hz). (Left) Displays the main effect of surface. Grey filled bar represents collapsed firm conditions and the hatched bar represents collapsed foam conditions. (Right) Displays the main effect of vision. Colours represent collapsed visual conditions as indicated in the legend. Standard error bars are displayed. Significance is indicated between sensory conditions. (*p<0.005, **p<0.001). 51

Figure 19: The Low and High Frequency Control Framework 72

Figure 20: This figure displays the FSCF-predicted responses (left) and the actual results (right) for the ultra-low frequency band (0-0.1Hz) for AP COP. To interpret this figure, the condition on the y-axis is compared to the subsequent condition on the x-axis. The legends indicate both the condition and the direction of change. Hatched boxes indicate foam surface conditions. A single arrow indicates a predicted increase or decrease, whereas a double arrow indicates a stronger predicted change supported by changes in more than one variable. 89

Figure 21: This figure displays the FSCF-predicted responses (left) and the actual results (right) for the low frequency band (0.1-0.5Hz) for AP COP. To interpret this figure, the condition on the y-axis is compared to the subsequent condition on the x-axis. The legends indicate both the condition and the direction of change. Hatched boxes indicate foam surface conditions. A single arrow indicates a predicted increase or decrease, whereas a double arrow indicates a stronger predicted change supported by changes in more than one variable. 89

Figure 22: This figure displays the FSCF-predicted responses (left) and the actual results (right) for the medium frequency band (0.5-1Hz) for AP COP. To interpret this figure, the condition on the y-axis is compared to the subsequent condition on the x-axis. The legends indicate both the condition and the direction of change. Hatched boxes indicate foam surface conditions. A single arrow indicates a predicted increase or decrease, whereas a double arrow indicates a stronger predicted change supported by changes in more than one variable. 90

Figure 23: This figure displays the FSCF-predicted responses (left) and the actual results (right) for the high frequency band (1-5Hz) for AP COP. To interpret this figure, the condition on the y-axis is compared to the subsequent condition on the x-axis. The legends indicate both the condition and the direction of change. Hatched boxes indicate foam surface conditions. A single arrow indicates a predicted increase or decrease, whereas a double arrow indicates a stronger predicted change supported by changes in more than one variable. 90

Figure 24: This figure displays the FSCF-predicted responses (left) and the actual results (right) for the ultra-low frequency band (0-0.1Hz) for AP COM. To interpret this figure, the condition on the y-axis is compared to the subsequent condition on the x-axis. The legends indicate both the condition and the direction of change. Hatched boxes indicate foam surface conditions. A single arrow indicates a predicted increase or decrease, whereas a double arrow indicates a stronger predicted change supported by changes in more than one variable. 91

Figure 25: This figure displays the FSCF-predicted responses (left) and the actual results (right) for the low frequency band (0.1-0.5Hz) for AP COM. To interpret this figure, the condition on the y-axis is compared to the subsequent condition on the x-axis. The legends indicate both the condition and the direction of change. Hatched boxes indicate foam surface conditions. A single arrow indicates a predicted increase or decrease, whereas a double arrow indicates a stronger predicted change supported by changes in more than one variable. 91

Figure 26: This figure displays the FSCF-predicted responses (left) and the actual results (right) for the medium frequency band (0.5-1Hz) for AP COM. To interpret this figure, the condition on the y-axis is compared to the subsequent condition on the x-axis. The legends indicate both the condition and the direction of change. Hatched boxes indicate foam surface conditions. A single arrow indicates a predicted increase or decrease, whereas a double arrow indicates a stronger predicted change supported by changes in more than one variable. 92

Figure 27: This figure displays the FSCF-predicted responses (left) and the actual results (right) for the medium frequency band (0.5-1Hz) for AP COM. To interpret this figure, the condition on the y-axis is compared to the subsequent condition on the x-axis. The legends indicate both the condition and the direction of change. Hatched boxes indicate foam surface conditions. A single arrow indicates a predicted increase or decrease, whereas a double arrow indicates a stronger predicted change supported by changes in more than one variable. 92

Figure 28: Relative frequency composition of the AP COP for the low frequency domain (0-0.5Hz). Solid bars are firm surface conditions. Hatched bars are foam surface conditions. Colours represent visual conditions as indicated in the legend. Standard error bars are displayed. Significance is indicated between sensory conditions. (*p<0.005, **p<0.001). 94

Figure 29: Relative frequency composition of the AP COP for the high frequency domain (0.5-5Hz). Solid bars are firm surface conditions. Hatched bars are foam surface conditions. Colours represent visual conditions as indicated in the legend. Standard error bars are displayed. Significance is indicated between sensory conditions. (*p<0.005, **p<0.001). 96

List of Abbreviations

AMP ..... Amplified Optic Flow

AP ..... Anterior Posterior

BOS ..... Base of Support

CNS ..... Central Nervous System

COM ..... Centre of Mass

COP ..... Centre of Pressure

CTSIB ..... Clinical Test of Sensory Interaction on Balance

EC ..... Eyes Closed

EMG ..... Electromyography

EO ..... Eyes Open

FSCF ..... Frequency-Specific Sensory Contribution Framework

HMD ..... Head Mounted Display

ML ..... Medial Lateral

MVC ..... Maximum Voluntary Contraction

OF ..... Optic Flow

PNS ..... Peripheral Nervous System

SOT ..... Sensory Organization Test

SR ..... Sway-Referenced

VR ..... Virtual Reality

Chapter 1: Introduction

Maintaining balance is essential in daily living. To stand upright, balance control systems must adapt and adjust based on sensory information from the environment. During upright stance, balance is maintained using information from the visual, vestibular, and somatosensory systems [1,2]. When performing activities of daily living, it is necessary to integrate sensory information accurately to maintain balance. As part of this integration process, afferent signals from each system are weighted, or adjusted, according to their reliable contribution to balance control [2]. The integrated signal is then used to modulate and coordinate muscular responses within the biomechanical constraints of the body to maintain upright stance [3]. Investigation into how upright stance adapts under altered sensory environments is crucial in our understanding of postural control mechanisms, as manipulation of sensory information allows for the examination of how the nervous system maintains upright stance.

This thesis consists of five chapters. Chapter 1 includes a literature review outlining the concepts of upright stance, including the maintenance of balance, sensory integration and reweighting, as well as the frameworks that shape the current interpretations of sensory contributions to upright stance. Chapter 2 presents a detailed description of the thesis methodology and analysis. Chapter 3 presents the results of the thesis. Chapter 4 presents the discussion and interpretations of the thesis results. Chapter 5 provides conclusions of the results and a proposed framework for interpreting frequency data associated with upright stance.

1.1 Maintenance of Upright Stance

Upright stance occurs when a person maintains a standing posture by controlling their centre of mass (COM) within the base of support (BOS) [4]. The COM is the point representing the weighted average position of all the mass in the body [4]. The BOS is the area on the ground enclosed by all points of contact between the body and the support surface [4]. The centre of pressure (COP) is the point of application of the resultant ground reaction force acting between the body and the support surface; its displacement represents the net neuromuscular response used to maintain upright stance [4]. The relationship that maintains the COM within the BOS is an in-phase relationship between the positions of the COM and the COP, in which the COP constrains the COM within the BOS [4,5]. The COP-COM relationship is regulated through sensory feedback loops, where information from the peripheral nervous system (PNS) is processed by the central nervous system (CNS) [6]. Sensory feedback loops operate both reactively and predictively to modulate muscular responses to regulate body movement to maintain upright stance [1,7]. The CNS selects the appropriate muscle activation patterns to implement postural corrections via these sensory feedback loops [8]. Together, these sensory feedback loops and motor responses maintain balance by coordinating COP adjustments that corral the COM within the BOS.

1.2 Balance Tests & Tools for Balance Assessment

Assessing the changes in upright stance behaviour during the controlled alteration of sensory information is crucial to understanding the ways in which we maintain balance in complex, dynamic real-world settings. Determining whether adaptations in postural sway reflect sensory-specific contributions or broader adaptations in postural control strategies is a fundamental component of this understanding. Across the literature, measuring the COP and COM during systematic alteration of afferent sensory information allows for analysis and

interpretation of the sensory contributions to balance; however, methods for these manipulations vary and have been limited in terms of technological accessibility.

The "Sensory Organization Test" (SOT) is a standardized functional assessment used to evaluate sensory reweighting and integration across the visual, vestibular, and somatosensory systems during upright stance [9]. The SOT consists of six conditions that systematically alter or remove sensory inputs by manipulating the visual surround and support surface [10]. The six conditions include three visual manipulations: eyes open (EO); eyes closed (EC); and sway-referenced (SR) vision, each performed on both a firm and SR tilting platform. Sway-referencing creates unreliable sensory input by moving the visual scene or support surface in direct proportion to a person's body sway, thereby reducing or eliminating relative motion cues required for accurate sensory feedback. Specifically, SR vision is achieved by having a visual scene move synchronously with postural sway and removes motion cues from the visual environment. Similarly, a SR platform manipulates somatosensory feedback by moving in proportion (1:1) to the participant's COM to eliminate angular ankle joint displacement and reduce the reliability of proprioceptive cues about body motion [11]. This controlled manipulation allows for the examination of how individuals reweight sensory inputs to maintain upright stance under unreliable sensory conditions. Until recently, SOTs have been limited to the anterior-posterior (AP) direction using NeuroCom or EquiTest systems [10,12]. These systems are costly and proprietary, making the replication of results inaccessible. The inconvenience of these systems creates a barrier to assessing the benefits of this test, thus creating a need for alternative methodology to test upright stance under altered sensory environments.

Another way in which sensory contributions to upright stance are tested is through the Clinical Test of Sensory Interaction on Balance (CTSIB). The conditions of the CTSIB examine

the same sensory manipulations as the SOT in a way that is feasible for clinical and research applications due to minimal and accessible equipment. The six conditions include three visual manipulations: EO; EC; and SR vision with the use of a dome placed over the participant's head, each performed on both a firm and a foam surface [13,14]. Standing on a foam surface affects somatosensory input to joint receptors and cutaneous mechanoreceptors as pressure distribution under the feet is altered relative to a firm surface, thereby reducing the reliability of proprioceptive feedback [15,16]. Further, the foam surface increases the magnitude of feedforward muscle activity in comparison to a firm surface, as the compliant surface generates earlier activation of dorsi- and plantar flexor muscles [16–18]. Thus, a foam surface impacts the afferent somatosensory information and subsequent postural control strategies to maintain upright stance. Despite the ease of administration, neither the SOT nor CTSIB leverage the advancements in modern day technology to replicate real-world environments in a controlled setting.

Virtual reality (VR) provides an opportunity to administer a wide range of visual conditions in a controlled manner by creating realistic, three-dimensional visual scenes with the capacity to manipulate real-time visual input and feedback during upright stance [19]. Delivered through a head-mounted display (HMD), VR allows participants to be fully immersed in dynamic environments that closely mimic real-world conditions. The use of VR in balance research has been validated across a range of participants, including healthy young and older adults, as well as clinical populations [20]. When comparing current VR technology to real-world balance, there has been no reported difference in upright stance between real-world and VR photorealistic environments [19]. Importantly, VR enables fine control of visual feedback, making it an effective tool for investigating visual contributions to upright stance [21]. The addition of VR

to SOT/CTSIB approaches can broaden our understanding of how visual information impacts the maintenance of upright stance by including visual manipulations within photo-realistic scenes.

1.3 Sensory Contributions to Upright Stance

1.3.1 The Role of the Visual System on the Control of Upright Stance

Visual information contributes to upright stance by providing external spatial reference cues about the body's orientation and motion relative to the surrounding environment. These signals inform the CNS of postural sway, interpret self-motion, and adjust postural responses when maintaining upright stance. Visual cues such as optic flow, retinal slip, and visual fixation allow the nervous system to estimate self-motion and distinguish movement of the body from movement of the visual scene [22]. Visual information is first processed in the retina and transmitted through the optic nerve, lateral geniculate nucleus, and primary visual cortex before being further processed in dorsal stream visual areas involved in motion perception and visually guided action [23]. Visual signals are integrated with vestibular and somatosensory cues to determine motion caused by body sway, head, or environmental motion [1]. However, visual information does not inform where the body is relative to the support surface or gravity, a responsibility of the somatosensory and vestibular systems [22].

Optic flow (OF) refers to the pattern of visual motion generated on the retina by the relative movement between the observer and the surrounding environment, which can be a result of self-motion or environmental movement [24]. OF is essential for perceiving the environment and one's position within it, as motion cues from both objects and self-movement allow for rapid and accurate estimation of direction [25]. Work that investigated the effects of amplified OF on upright stance has shown that amplified OF results in decreased sway amplitude and increased frequency

composition of COP displacement and head position in the AP direction [26,27]. Visual conflicts such as SR visual environments are known to increase postural sway in healthy populations [22,28]. Additionally, removed visual information (EC) has been shown to increase sway, giving evidence to the importance of the visual system in the maintenance of upright stance [29].

Typically, visual contributions to balance have been associated with slow, low frequency postural sway. Specifically, frequency-domain analyses of COP signals during quiet stance suggest that visual contributions to balance are most strongly reflected in COP power below 0.1 Hz [22,30–32]. This evidence is derived from observed shifts in COP frequency content toward frequencies above 0.1 Hz during an EC condition compared to "normal" visual conditions (EO) [33].

1.3.2 The Role of the Vestibular System on the Control of Upright Stance

The vestibular system is responsible for providing information about three-dimensional linear and angular acceleration in relation to gravity via the semi-circular canals and the otolith organs [34]. The afferent signal from the vestibular apparatus is transmitted through the vestibular nerve to the vestibular nuclei and cerebellum. These regions integrate vestibular input with visual and somatosensory information before sending descending motor commands through vestibulospinal and reticulospinal pathways to the spinal cord. These pathways influence trunk, limb, and neck muscle activity to maintain upright posture and stabilize the head and body [35,36].

The vestibular apparatus are located within the inner ear on both sides of the head. There are three mutually orthogonal semi-circular canals called the horizontal, posterior, and anterior canals, which are responsible for the detection of angular head acceleration [37]. The two otolith organs in the inner ear, the utricle and saccule, are responsible for detecting linear accelerations

of the head. The sensitivity of the semi-circular canals is 0.05 deg/sec^2, sufficient to detect the minute angular head accelerations that occur during quiet stance [38]. An angular head acceleration of 0.05 deg/sec^2 reflects a gradual change in head rotation, consistent with slow motion during upright standing relative to the larger rotations and accelerations common during voluntary head movement. The otolith organs are sensitive to linear movement at approximately 0.059 m/s^2 [39]. Recent work has shown that short latency reflexes and small transient sway are driven by the otolith organs, while medium latency responses and larger sway are driven by the semi-circular canals [40]. This work provides evidence that the vestibular system can influence both slow and fast upright stance control.

Head displacements produce distinct postural and muscular responses to maintain the position of the COM with relation to the motion and orientation of the head [28]. The contribution of the vestibular system to upright stance is evident when head displacement is induced in those with vestibular loss and during targeted perturbations. Vestibular perturbations preferentially activate the head and neck muscles with smaller, coordinated adjustments than in the trunk and lower extremities [41]. The vestibular contributions to balance are also apparent in galvanic-electrical stimulation of the vestibular apparatus, which evokes organized postural responses depending on the stimulus polarity and head orientation [42]. Vestibular input is commonly hypothesized to contribute to low-to-mid frequency postural control, particularly within the 0.1–1Hz range [43]. The latency of vestibular-evoked responses are comparable to that of somatosensory reflexes, providing rapid feedback [40]. Both are critical for balance control, yet their functional outputs differ, as head displacements are the driver for fast vestibular responses [41]. Vestibular information is important for estimating head and upper-body motion relative to gravity, thereby contributing to spatial orientation in the maintenance of upright stance.

1.3.3 The Role of the Somatosensory System on the Control of Upright Stance

The somatosensory system is the body's sense of touch, temperature, pain, and position. It relies on skin mechanoreceptors, deep tissue pressure receptors, muscle spindles, Golgi tendon organs, and joint receptors [44]. This information is transmitted through peripheral afferent pathways to the spinal cord, where it contributes to reflexive postural adjustments and can be transmitted to supraspinal structures such as the brainstem, cerebellum, thalamus, and somatosensory cortex. In these higher brain areas, somatosensory information contributes to sensory integration, body orientation, and the generation of coordinated postural responses [1,45]. Somatosensory input from the feet and lower limbs informs the CNS of body orientation and support surface conditions, enabling precise modulation of postural muscle activity [4]. It is also evident in the literature that trunk proprioception is vital to controlling upright stance. The reduction in function of the somatosensory system, via ischemic hypoxia of the feet and ankles, resulted in postural control strategies that relied more heavily on trunk related movement [28]. Overall, the literature suggests that the somatosensory system is multifaceted and relays balance relevant information through the CNS from both the trunk and lower body.

When support surface translations, rotations, or sway-referencing platforms induce unreliable somatosensory information, postural sway increases, thought to be related to a greater dependence on visual and vestibular cues through the sensory reweighting process [1,41]. The somatosensory system uses feedback from muscle–tendon stretch and soft tissue deformation of the ankle to generate reflex-driven adjustments to correct sway, accounting for both low and high frequency postural adjustments [46]. Low and high frequency postural control mechanisms parallel behaviour of fast and slow adapting mechanoreceptors in the plantar surface [47], while muscle spindle and stretch reflex loops induce rapid corrections greater than 1Hz [28,48]. This indicates that

the somatosensory system contributes not only to rapid, high frequency corrections, but also plays a role in slower, low frequency sway regulation.

1.4 Sensory Integration & Reweighting

The CNS must process balance relevant sensory information from afferent signals from the PNS to maintain upright stance [6]. This closed-loop process regulates balance through neural control mechanisms, whereby sensory inputs are integrated and weighted according to their reliability to modulate motor outputs and muscular activity [1]. The Independent Channel Theory postulates how weighting of sensory input occurs, wherein the reweighting process is a weighted sum of information dictated by amplitude, velocity, and the reliability of sensory information [1,2,6,49–51]. This theory is central to the concept of sensory reweighting and how sensory systems contribute to specific frequencies of balance control; it suggests that visual, vestibular, and somatosensory systems independently provide information about the environment, head orientation, body position, and movement relative to the support surface [1]. Together, these sensory inputs are processed within the CNS and are dynamically reweighted to maintain postural stability under changing environmental conditions [1].

The CNS regions associated with sensory integration and reweighting are the spinal cord, brainstem, cerebellum, and cerebral cortex. The spinal cord receives afferent sensory information from the body and can generate a reflexive motor command or transmit information to higher-order brain centres. At the spinal level, proprioceptive, cutaneous, and muscle-tendon afferents contribute to rapid reflexive postural responses [52,53]. In a reweighting context, the spinal cord rapidly modifies muscle activation patterns when input from sensory modalities changes and motor adjustments are necessary [52]. The brainstem aids in relaying and integrating sensory information, including vestibular and reticular pathways, while cerebellar mechanisms refine and

adapt balance control [54]. The brainstem sends descending motor commands from the cortex and reflexively to the spinal cord via the vestibulo-, reticulo-, tecto-, and rubro-spinal tracts [2,55]. When sensory reliability is altered, such as when vision is removed or a support-surface tilts, the brainstem adjusts the gain and integration of the postural reflex pathway [34]. Further, descending pathways from the brainstem contribute to anticipatory postural adjustments and postural reflexes [56].

The cerebellum plays a crucial role in integrating balance-relevant sensory information and coordinating postural responses [57]. Specific regions of the cerebellum influence its contributions to balance, evident through the assessment of patients with cerebellar atrophy and lesions [58]. Anterior lobe atrophy of the cerebellum produces a high frequency sway tremor in the AP direction. The anterior lobe is part of the spinocerebellum and receives sensory afferents from the spinal cord. The flocculonodular lobe is part of the vestibulocerebellum, which receives sensory afferents from the vestibular system. When there are lesions on the flocculonodular lobe, low frequency, multi-directional sway is produced [59]. When sensory conditions change, such as standing on a compliant surface versus solid ground, the cerebellum can dynamically adapt motor commands based on afferent sensory information as well as predictively through the use of the efference motor copy [1,34].

The cerebral cortex, specifically the parietal lobe, integrates visual, proprioceptive, and vestibular inputs to guide context-specific motor adjustments. The parietal lobe is central in sensorimotor integration, and functional magnetic resonance imaging research has shown that parietal activity increases with conflicting sensory information or changes in its reliability [60,61]. For successful sensory and motor integration to maintain upright stance, these components of the

CNS must effectively receive, integrate, and process afferent information to provide effective efferent motor commands.

1.5 Frequency-Specific Sensory Contribution Framework

The Frequency-Specific Sensory Contribution Framework (FSCF) provides a foundation to interpret how each sensory system may influence postural control within specified frequency ranges, or bands [32]. The FSCF uses four frequency bands defined as visual, vestibular, cerebellar, and proprioceptive contributions to balance, respectively [31–33,48,54,62], as shown in Figure 1. When interpreting or analyzing the balance data associated with the sensory specific frequency contributions to balance, the FSCF-defined frequency bands are used and described as: ultra-low (0.0-0.1Hz); low (0.1-0.5Hz); medium (0.5-1.0Hz); and high (1.0-5.0Hz). The changes in COP frequency content in the sagittal plane under sensory manipulation are the evidence used to define the frequency bands [31–33,43,48,54].

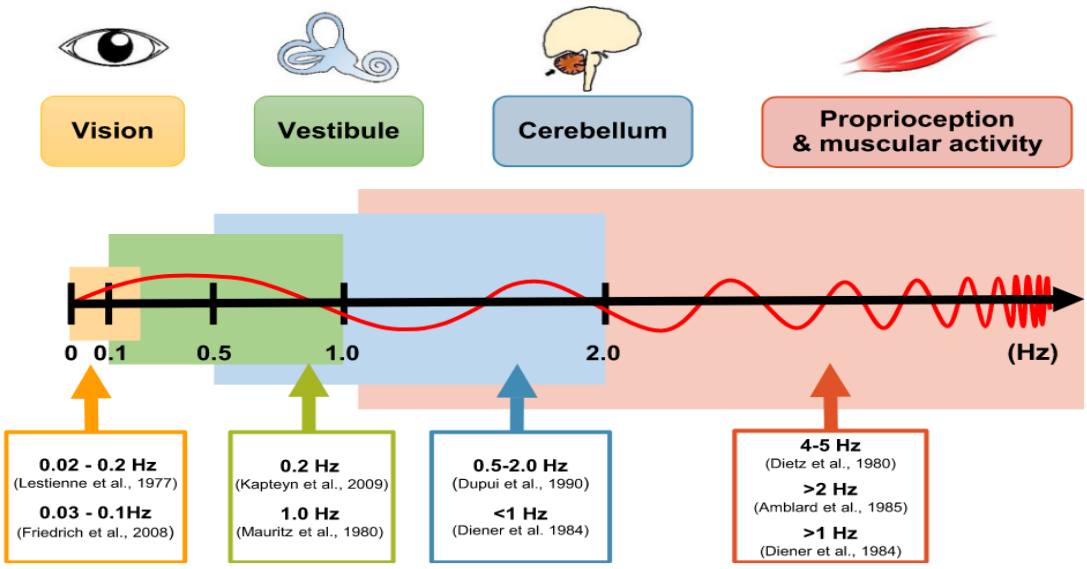

***Figure 1**: Frequency band of the sensory systems. Reproduced from Lin et al. (2019), under the Creative Commons Attribution 4.0 International Licence. No changes were made.*

1.6 Current Research Gap & Significance

Sensory contributions to upright stance have been studied using a variety of techniques across different experimental contexts. However, interpretation of the sensory contributions to balance have been limited to relating sensory contributions to FSCF-hypothesized frequency bands, which do not encompass the dynamic interactions between sensory reweighting and frequency-related control strategies. It is important to continue developing a mechanistic understanding of sensory contributions to upright stance to build a comprehensive framework of how upright stance adapts to improve the interpretation of balance data.

The sensory contributions to upright stance show evidence of a context-dependent relationship with COP frequency. This context-dependent relationship is not reflected by the current FSCF, as sensory information has been shown to extend beyond the hypothesized frequency bands associated with sensory systems. As mentioned in *section 1.3.1*, studies manipulating OF during upright stance have shown that amplified OF results in decreased sway amplitude and increased frequency composition of COP displacement and head position in the AP direction [26,27]. An increase in COP frequency during amplified OF suggests that visual contributions to balance extend beyond the ultra-low (0-0.1Hz) frequency band, demonstrating a context-dependent relationship between COP frequency and balance-relevant visual information during the maintenance of upright stance. Thus, the FSCF may not be a robust model to accurately describe the visual contributions to upright stance, calling into question its integrity for all sensory-related contributions to the maintenance of upright stance.

It is postulated that the vestibular contribution to balance can effectively encode sensory information above 0.1 Hz [63]. As mentioned in *section 1.3.2*, vestibular input is commonly hypothesized to contribute to low-to-mid frequency postural control, particularly within the 0.1–

1 Hz range [43]. Standing on a compliant foam surface with EC has traditionally been used as a vestibular-challenging balance condition where visual feedback is removed and somatosensory feedback from the support surface is unreliable, increasing reliance on vestibular information. The frequency characteristics between the vestibular-challenging balance condition compared to a control task, in which a person is standing with intact sensory input, shows a shift of frequency to between 0.1-1Hz [43,64,65]. This is evidenced by COP frequency power increasing within the defined low-medium frequency band (0.1-1Hz) associated with vestibular contributions to balance [66,67]. However, the low-to-medium frequency range should not be interpreted as representing isolated vestibular input, as the maintenance of upright stance reflects the integrated weighting of visual, vestibular, and somatosensory cues.

Furthermore, the FSCF suggests that somatosensory contributions dominate higher-frequency sway (>1 Hz), based on observations that frequency power increases when visual or vestibular inputs are disrupted [32,62]. However, studies analyzing upright stance show that there is an increase in mean power frequency on foam relative to a firm surface [27,68]. Thus, an increase in frequency with unreliable somatosensory information demonstrates that the somatosensory system is not solely relied upon for higher frequencies of balance control [69].

The FSCF does not account for sensory reweighting mechanisms, which display a non-linear pattern evident through the scaling of postural responses, asymmetric dynamics, and internal thresholds [2,50,70,71]. Crucially, the FSCF does not include other balance relevant variables, such as kinematics and muscle activity, to define these frequency-specific sensory contributions to balance. Kinematic variables such as COM motion reflect whole body displacement. The displacement of the COM is corralled by the COP. However, during upright stance altered sensory information may modify the frequency of the COM–COP relationship, reflecting

adaptations in control strategy that are missed in the current FSCF [4,72]. Further, the frequency of muscle activity may differ from COP and can provide insight into the frequency-specific sensory contributions to upright stance. COM and muscular activity are fundamentally different than the COP and reflect different processes of upright stance maintenance. Muscular activity is the output of the motor control system to generate movement. The COP is the resultant ground reaction force acting between the body and the support surface, and its displacement represents the net neuromuscular response. The COM is the point representing the weighted average position of all the mass in the body. Changes in COM position represent the displacement of the entire body during movement. These variables represent distinct outcomes and are crucial in the maintenance of upright stance. Understanding how the frequency relationship between these variables changes under altered sensory information are not reflected by the FSCF. Thus, a more robust frequency-specific control framework encapsulating variables during the entire upright stance process will improve interpretations of frequency data.

1.7 Purpose

The purpose of this thesis was to critically examine and challenge the FSCF to assess its robustness to explain kinetic, kinematic, and muscle activity outcomes during sensory manipulations. Ultimately, this work aimed to improve the characterization of how sensory information shapes and regulates balance control. Specifically, this thesis investigated the frequency outcomes of kinetic, kinematic, and muscle activity variables during upright stance to further develop a more robust understanding of the frequency-specific sensory contributions to balance. A novel Virtual Reality-Sensory Interaction Balance Test was used to administer controlled alterations of visual information and somatosensory information during upright stance. Advancing our understanding of these the frequency-related outputs will facilitate the

development of a comprehensive framework for understanding how postural dynamics adapt and improve the interpretation of balance data.

1.8 Research Question & Hypothesis

The research question for this thesis was: how does manipulating sensory information alter the frequency-specific characteristics of postural control?

Specifically:

1) What is the change in AP COP, AP COM, and right soleus muscle activity total band power between sensory conditions?

2) How does the relative percent contribution of AP COP, AP COM, and right soleus muscle activity change in each frequency band in comparison to total signal power across sensory conditions?

It was hypothesized that:

1) Total band power would differ between sensory conditions for all dependent variables (AP COP, AP COM, and right soleus muscle). Specifically, sensory conditions with less reliable and/or removed sensory information would have an increased total band power and amplified visual information would reduce total band power.

2) There would be a compositional shift in frequency power when sensory information is manipulated for all dependent variables (AP COP, AP COM, and right soleus muscle activity). It was hypothesized that when somatosensory information was made unreliable, frequency composition would decrease below 1Hz, reflective of a shift outside of the high frequency band (1-5Hz). It was also hypothesized that when visual information is amplified, frequency

composition would display an increase in the medium (0.5-1Hz) and high frequency (1-5Hz) bands compared to normal vision. Further, it was hypothesized that there would be no difference in frequency composition between removed or unreliable visual conditions. However, removed and unreliable visual conditions would display an increased frequency composition in the medium (0.5-1Hz) and high (1-5Hz) frequency bands compared to normal and amplified visual information. Lastly, it was hypothesized that when multiple sensory systems are manipulated, there would be a disproportionate shift of frequency composition, which relates to task difficulty.

Chapter 2: Methods

2.1 Participants

Healthy young adults between the ages of 18 and 40 were recruited for this study. Participants self-reported their height and weight. The exclusion criteria included any known balance, neurological or musculoskeletal impairments that may affect the participant's ability to complete the tasks. All participants provided written informed consent approved by the York University Research Ethics Board (certificate #e2019-367).

2.2 Procedure

Participants were exposed to eight conditions in a randomized order for a duration of two minutes and completed each condition once (Table 1). Prior to stepping onto the force plate, all kinematic and electromyography (EMG) sensors were placed (*sections 2.4.1 & section 2.4.3*). Maximum voluntary contractions (MVC) were performed for the muscles of interest (*section 2.4.3*). MVCs were performed for all muscles three times for five seconds each, with one minute of rest between efforts to account for fatigue. Participants were verbally motivated while they executed an isokinetic contraction against a fabric band for each of the muscles of interest. Specifically, the right soleus MVC was recorded while the participants sat on top of a massage table with their knee hanging off the edge of the table at 90 degrees. Participants pushed down with their right foot onto a fabric band, with their ankle at 90 degrees. Resistance was generated by the researcher resisting the downward force of the participant.

On the force plate, foot placement was standardized to shoulder width and marked with tape to ensure consistency across conditions. A foam pad (dimensions: 10 × 61 × 46 cm; density: 25 kg/m^3) was placed on top of the force plate for four out of the eight conditions to alter

somatosensory feedback from the feet and ankles. The compliant surface deformed under the feet, changing plantar pressure distribution and reducing the reliability of cutaneous and proprioceptive information used to detect body sway. Foot placement on the foam surface was also standardized to shoulder width and marked.

A spotter stood next to the participant during the experimental trials to ensure safety; no safety harness was worn during the duration of this experiment. The HMD was placed on the participant after they stepped onto the force plate. Participants wore the HMD for the entire duration of the experimental portion of the study, unless otherwise instructed to adjust between firm and foam surfaces, or if the participant needed a break. At the end of each experimental condition, participants were asked if they required a break before continuing. If requested, a break lasted a minimum duration of two minutes either standing or seated off the force plate. Participants were periodically asked to close their eyes while the visual scene was being switched between conditions to prevent disorientation. Before starting the experimental conditions, participants were familiarized with the realistic virtual environment as well as the firm and foam surface. Familiarization was confirmed verbally after a minimum duration of one minute on both firm and foam surfaces. The experimental design is displayed in Figure 2.

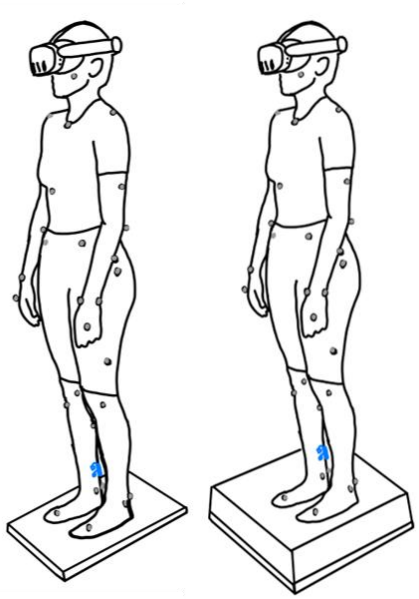

Figure 2: *Experimental set-up with firm (left) & foam (right) surfaces (EMG sensors for the left TA and right soleus are displayed. Tape markings are not displayed).*

2.3 Experimental Conditions

The list of conditions and sensory manipulations are listed in Table 1. There were eight different conditions, which consisted of a combination of four visual and two surface conditions.

Table 1: *A list of the conditions with their corresponding sensory manipulation in the VR-SIBT.*

Condition (C)	Vision	Somatosensory
1	Realistic / Normal (EO)	Firm / Normal
2	Eyes Closed / Removed (EC)	Firm / Normal
3	Amplified Optic Flow (AMP)	Firm / Normal
4	Sway-Referenced Vision / Unreliable (SR)	Firm / Normal
5	Realistic / Normal (EO)	Foam / Unreliable
6	Eyes Closed / Removed (EC)	Foam / Unreliable
7	Amplified Optic Flow (AMP)	Foam/ Unreliable
8	Sway-Referenced Vision / Unreliable (SR)	Foam / Unreliable

2.3.1 Virtual Reality Scene

The realistic VR scene was set in an art gallery with a fixation point (red square) in the centre of the screen (Figure 3). The HMD showed one of four visual conditions, three of which displayed the realistic art gallery scene: realistic OF (EO), blacked-out screen (EC), amplified OF (4x) (AMP), or visual sway-referencing (0x) (SR). The realistic OF condition (C1/C5) provided 1:1, real-world coupling between head motion and visual motion. The blacked-out screen (C2/C6) removed visual information, and participants were asked to also close their eyes to ensure there was no visual input; participants self-reported that their eyes were closed. Amplified OF (C3/C7) used real-time head motion to provide four times the amount of scene motion in two degrees of freedom: the AP and medial-lateral (ML) directions. Scene motion in the other degrees of freedom remained 1:1 to real head motion. Sway-referenced vision (C4/C8) locked the image to head motion in all six degrees of freedom to remove motion cues from the visual environment.



Figure 3: *Participants' view inside the HMD of the realistic art gallery scene.*

2.4 Measurements

2.4.1 Kinetics

Participants stood on a single force plate (AMTI, OPITMA OR6-OP, USA); signals were sampled at 1000Hz and recorded through VICON Nexus 2 software to collect ground reaction forces and moments (Figure 2), and processed in MATLAB (The MathWorks Inc., USA). Kinetic data were low-pass filtered with a fourth-order dual-pass Butterworth filter and a 5 Hz cut-off frequency. Kinetic data were also bias-removed. [26]. Kinetic data were used to calculate COP displacements in the AP direction.

2.4.2 Kinematics

VICON Nexus 2 software recorded kinematic data from 46 reflective markers, sampled at 100Hz and processed in MATLAB (The MathWorks Inc., USA). Ten cameras were placed around the room to capture motion from the reflective markers. The kinematic markers were placed bi-laterally on the following anatomical landmarks: the head (zygomatic bone and occipital bone), acromion process, upper arm on the humerus, olecranon process, lateral aspect of the ulna, styloid processes of the radius and the ulna, distal end of the 3rd metacarpal, anterior superior iliac spine, posterior superior iliac spine, greater trochanter, lateral aspect of the femur, medial and lateral condyles of the knee, lateral aspect of the tibia, medial and lateral malleoli of the ankle, calcaneus, and distal end of the 3rd metatarsal. There were five midline markers placed on the seventh cervical vertebra, tenth thoracic vertebra, right scapula, jugular notch, and xiphoid process (Figure 2). The displacements of individual markers were used to quantify whole body and segmental COM. Kinematic data were low-pass filtered with a fourth-order dual-pass Butterworth filter and a 5 Hz cut-off frequency. Kinematic data were also bias-removed.

2.4.3 Electromyography

Eight EMG sensors were placed on the participant to record bilateral muscle activity of the lateral soleus, medial gastrocnemius, tibialis anterior and the medial gluteus muscles. EMG activity was recorded using the Noraxon EMG system and sampled at 2000Hz through the Vicon Nexus 2 software (Noraxon, USA). The Noraxon EMG amplifier has a built-in bandpass filter at 10-500Hz. EMG data were processed using a zero-phase digital filtering pipeline to remove noise and isolate the physiological EMG bandwidth. A second-order Butterworth notch filter at 60 Hz was applied to eliminate electromagnetic noise, followed by a fourth-order dual-pass Butterworth bandpass filter between 30 and 500 Hz to remove low frequency motion artifacts and high frequency noise. The filtered signals were full-wave rectified and then a low-pass fourth-order dual-pass Butterworth filter with a 5 Hz cutoff was applied to create a linear envelope to represent the overall muscle activation profile. The resulting linear envelope was used for subsequent analyses of muscle activity across experimental conditions [73,74]. EMG data were normalized to each participant's MVC to account for inter-individual variability. MVC procedure can be found in *section 2.2*.

2.5 Data Analysis

To critically examine the FSCF, the AP COP, AP COM, and right soleus muscle activity were used for analysis. The AP COP was used as the FSCF used evidence from AP COP data to determine the hypothesized frequency bands. The AP COM was used to see if there was a change in the relationship between AP COP and AP COM when sensory information was altered. Lastly, the right soleus was analyzed, as the right soleus is involved in continuous AP ankle control, crucial for the maintenance of upright stance. The recordings of the dependent variables were used to assess the changes in total band power and relative frequency contribution within the

defined frequency bands: ultra-low (0-0.1Hz), low (0.1-0.5Hz), medium (0.5-1Hz), and high (1-5Hz).

Frequency power was calculated from the processed AP COP, AP COM, and right soleus time series signals, using MATLAB's *bandpower* function [75]. This function estimates band-limited power using a modified periodogram, in which the time-domain signal is windowed before estimating the power spectrum. Frequency power was calculated within each predefined frequency band, and total band power was calculated as the sum of power across all frequency bands. The relative contribution of each frequency band was expressed as a percentage of total band power.

2.6 Statistical Analysis

Statistical analyses were run using SPSS software (IBM, USA). The Shapiro-Wilks test of Sphericity was used to evaluate normality for all outcome measures. Z-scores were calculated for each dependent variable, including total band power and relative frequency-band contributions derived from AP COP, AP COM, and right soleus EMG. The Z-scores were used to identify outliers, which were defined as ± 3 standard deviations from the mean; any outliers were winsorized to the 3 standard deviation value. Variables that remained non-normally distributed following winsorization were logarithmically transformed before statistical analysis. The α-level was set to 0.05 and Sidak corrections were utilized for multiple comparisons.

1) For each dependent variable (AP COP, AP COM, and right soleus EMG), four by two repeated-measures ANOVAs were conducted to assess whether total band power was affected by vision condition, surface condition, or the interaction between vision and surface. Within-subject factors were vision and surface. The primary outcomes were the main effect of vision and

surface, as well as the vision by surface interaction. These effects assessed differences in total band power among visual conditions, between firm and foam surfaces, and whether the effects of visual condition depended on the surface condition.

2) For each dependent variable (AP COP, AP COM, and right soleus EMG), four, four by two ANOVAs were conducted to assess whether frequency composition was affected by vision condition, surface condition, or the interaction between vision and surface within the four frequency bands. For each frequency band- ultra-low (0-0.1Hz), low (0.1-0.5Hz), medium (0.5-1Hz) and high (1-5Hz)- the within-subject factors were vision and surface. The primary outcomes were the main effects of vision and surface, as well as the vision by surface interaction. These effects assessed differences in relative frequency composition among visual conditions, between firm and foam surfaces, and whether the effect of visual condition depended on the surface condition for each frequency band.

Chapter 3: Results

3.1 Participant Demographics

Participant demographic information can be found in Table 2. All participants had normal or corrected-normal vision. AP COP and AP COM analyses were conducted from 32 participants. Right soleus EMG analyses were conducted on 30 participants, as two participants were excluded due to the absence of valid MVCs required for EMG normalization.

Table 2: *Participant demographics.*

Group size	32 (17 Female)
Age (years)	24.22 ± 3.47
Height (cm)	169.30 ± 10.56
Weight (kg)	74.21 ± 17.33

3.2 Summary Results Table

Table 3: *Results Summary of the AP COP, AP COM, and Right Soleus*

Domain	Signal	Interaction p	Interaction ηp²	Interaction Pattern	Vision p	Vision ηp²	Vision Differences	Surface p	Surface ηp²	Surface Direction
TOTAL BAND POWER (0–5 Hz)										
Kinetics	AP COP	0.006	0.123	Surface-dependent vision effect	<0.001	0.294	Reduced power during AMP	<0.001	0.671	Increase
Kinematics	AP COM	0.004	0.134	Surface-dependent vision effect	<0.001	0.223	Reduced power during AMP	<0.001	0.524	Increase
EMG	R Soleus	0.651	0.022	N/A	0.040	0.091	SR > EO	0.001	0.301	Increase
ULTRA-LOW FREQUENCY BAND (0–0.1 Hz)										
Kinetics	AP COP	0.277	0.040	N/A	<0.001	0.348	EO/AMP > EC/SR	<0.001	0.515	Decrease
Kinematics	AP COM	0.854	0.008	N/A	<0.001	0.414	AMP>EO>EC /SR	<0.001	0.362	Decrease
EMG	R Soleus	0.063	0.080	N/A	0.110	0.067	N/A	0.002	0.276	Decrease
LOW FREQUENCY BAND (0.1–0.5 Hz)										
Kinetics	AP COP	0.791	1.041	N/A	<0.001	0.457	EC/SR>EO>A MP	0.014	0.178	Increase
Kinematics	AP COM	0.961	0.003	N/A	<0.001	0.428	AMP>EO>EC /SR	0.001	0.285	Increase
EMG	R Soleus	0.007	0.128	Surface-dependent vision effect	<0.001	0.343	Reduced power during AMP	<0.001	0.483	Increase
MEDIUM FREQUENCY BAND (0.5–1.0 Hz)										
Kinetics	AP COP	0.004	0.135	Surface-dependent vision effect	<0.001	0.389	EC/AMP/SR >EO + AMP>SR	<0.001	0.566	Increase
Kinematics	AP COM	0.008	0.120	Surface-dependent vision effect	<0.001	0.283	EC/AMP/SR >EO	<0.001	0.591	Increase
EMG	R Soleus	0.667	0.018	N/A	0.016	0.111	EO<EC	<0.001	0.497	Increase
HIGH FREQUENCY BAND (1.0–5.0 Hz)										
Kinetics	AP COP	<0.001	0.190	Surface-dependent vision effect	<0.001	0.351	EC/AMP/SR >EO	<0.001	0.440	Increase
Kinematics	AP COM	<0.001	0.211	Surface-dependent vision effect	<0.001	0.248	EC/AMP/SR >EO	<0.001	0.350	Increase
EMG	R Soleus	0.367	0.036	N/A	0.002	0.155	EO<EC	<0.001	0.678	Increase

3.3 Total Band Power

The AP COP and AP COM showed a similar pattern in total band power across all eight conditions. This pattern evidenced differences between firm and foam surfaces of the same visual condition. Further, on the foam surface, AMP visual information reduced total band power compared to EO, EC and SR visual conditions. However, the total band power of the right soleus demonstrated an increased total band power on the foam surface, as well as a significant difference between only the EO and SR visual conditions. Overall, altered sensory conditions influenced the total band power associated with the maintenance of upright stance.

3.3.1 Kinetics

The analysis of AP COP total band power identified a main and interaction effect of surface and vision. Figure 4 shows the significant pairwise comparisons between the 8 conditions for the total band power of the AP COP.

There was an interaction effect between surface and vision for the total band power of the AP COP ($F(3,93)=4.363$, $p=0.006$, $\eta^2=0.123$). Post-hoc tests identified significant pairwise comparisons between C5 (EO on Foam) and C7 (AMP on Foam) ($p<0.001$), C6 (EC on Foam) and C7 (AMP on Foam) ($p<0.001$), as well as C8 (SR on Foam) and C7 (AMP on Foam) ($p<0.001$). C7 had less total band power than C5, C6, and C8. Furthermore, significant pairwise comparisons were identified between firm and foam surfaces within matched visual conditions, C1 (EO) and C5 (EO on Foam) ($p<0.001$), C2 (EC) and C6 (EC on Foam) ($p<0.001$), C3 (AMP) and C7 (AMP on Foam) ($p=0.008$) as well as C4 (SR) and C8 (SR on Foam) ($p<0.001$). The foam surface conditions (C5, C6, C7 and C8) had an increased total band power compared to the firm surface conditions with the same visual condition (C1, C2, C3, and C4). No other significant pairwise comparisons were identified.

The significant main effect of surface ($F(1,31)=63.337$, $p<0.001$, $\eta^2=0.671$) identified an increase in total band power for the foam surface compared to the firm surface. There was also a significant main effect of vision ($F(3,93)=12.904$, $p<0.001$, $\eta^2=0.294$). Post-hoc tests identified significant pairwise comparisons between: EO and AMP ($p=0.009$), EC and AMP ($p<0.001$), as well as SR and AMP ($p<0.001$). The total band power was lower in the AMP visual condition compared to the other visual conditions (EO, EC, and SR). No other significant pairwise comparisons were identified.

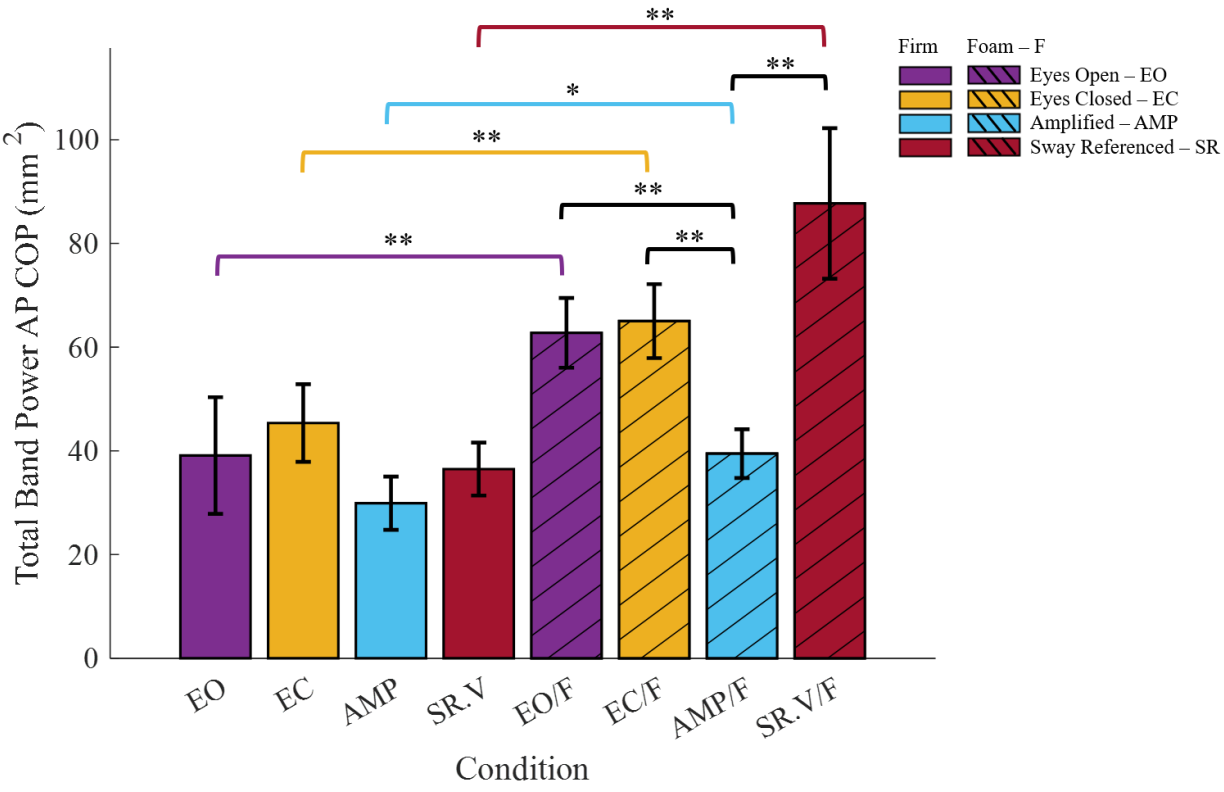

***Figure 4**: Total Band Power for AP COP. Solid bars are firm surface conditions. Hatched bars are foam surface conditions. Colours represent visual conditions as indicated in the legend. Standard error bars are displayed. Significance is indicated between sensory conditions. (*p<0.005, **p<0.001).*

3.3.2 Kinematics

The analysis of AP COM total band power identified a significant main effect of surface, and a significant interaction effect of surface and vision. Figure 5 shows the significant pairwise comparisons between the 8 conditions for the total band power of the AP COM.

There was an interaction effect between surface and vision for the total band power of the AP COM ($F(3,93)=4.812$, $p=0.004$, $\eta^2=0.134$). Post-hoc tests identified significant pairwise comparisons between differences between C5 (EO on Foam) and C7 (AMP on Foam) ($p<0.001$), C6 (EC on Foam) and C7 (AMP on Foam) ($p<0.001$), as well as C8 (SR on Foam) and C7 (AMP on Foam) ($p<0.001$). C7 had less total band power than C5, C6, and C8. Furthermore, significant pairwise comparisons were identified between firm and foam surfaces within matched visual conditions: C1 (EO) and C5 (EO on Foam) ($p<0.001$), C2 (EC) and C6 (EC on Foam) ($p<0.001$), as well as C4 (SR Vision) and C8 (SR on Foam) ($p<0.001$). The foam conditions (C5, C6, and C8) had an increased total band power compared to the firm conditions with the same visual condition (C1, C2, and C4), except for the AMP visual conditions (C3 and C7). No other significant pairwise comparisons were identified.

The main effect of surface ($F(1,31)=34.167$, $p<0.001$, $\eta^2=0.524$) identified an increase in total band power for the foam condition compared to the firm condition. The main effect of vision ($F(3,93)=8.879$, $p<0.001$, $\eta^2=0.223$) identified significant pairwise comparisons between: EO and AMP ($p=0,009$), EC and AMP ($p=0.002$), as well as SR and AMP ($p=0.001$). The total band power was lower in the AMP visual condition compared to the other visual conditions (EO, EC, and SR). No other significant pairwise comparisons were identified.

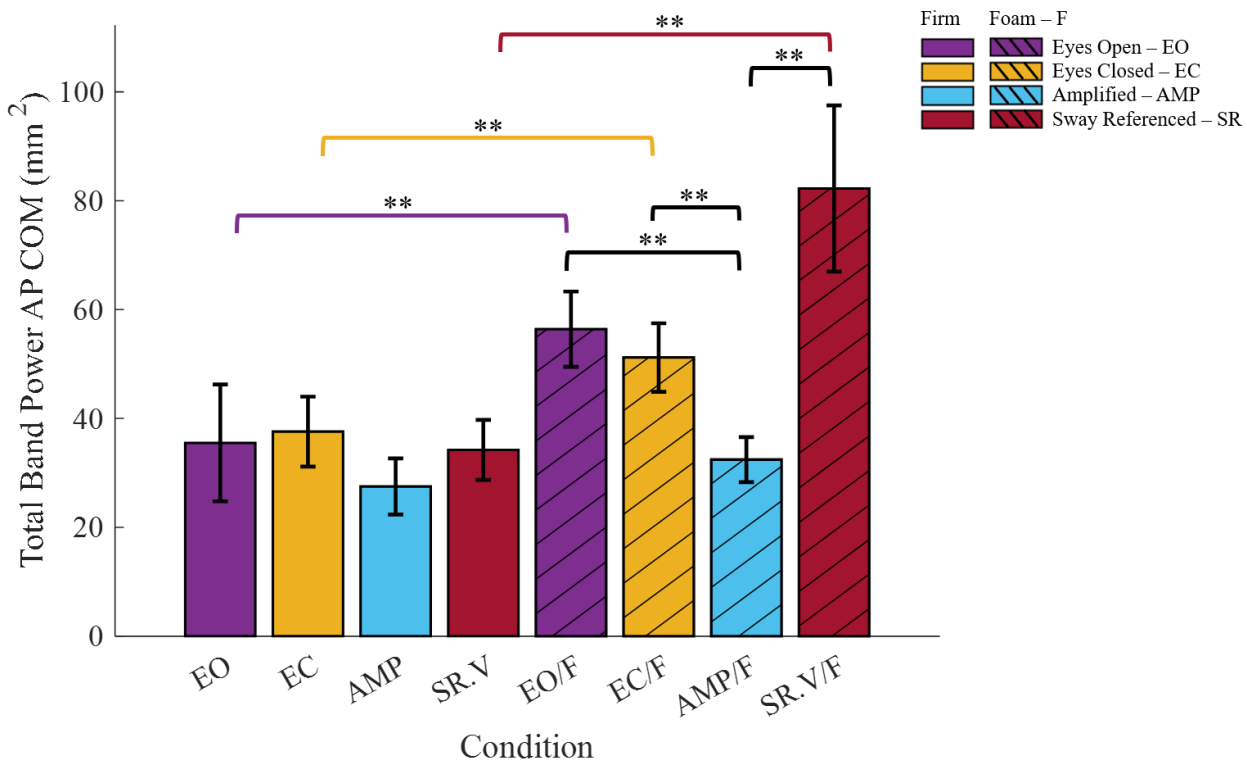

Figure 5*: Total Band Power for AP COM. Solid bars are firm surface conditions. Hatched bars are foam surface conditions. Colours represent visual conditions as indicated in the legend. Standard error bars are displayed. Significance is indicated between sensory conditions. (*p<0.005, **p<0.001).*

3.3.3 Electromyography

The analysis of right soleus total band power identified main effects of surface and vision. The main effect of surface ($F(1,29)=12.463$, $p=0.001$, $\eta^2=0.301$) identified an increase in total band power for the foam condition compared to the firm condition. The main effect of vision ($F(3,87)=2.890$, $p=0.040$, $\eta^2=0.091$) identified significant pairwise comparisons between: EO and SR ($p=0.039$). The total band power was higher for the SR condition compared to the EO condition. No other significant pairwise comparisons were identified. There was no interaction effect identified ($F(3,87)=0.651$, $p=0.651$, $\eta^2=0.022$). Figure 6 shows the significant main effects of surface and vision.

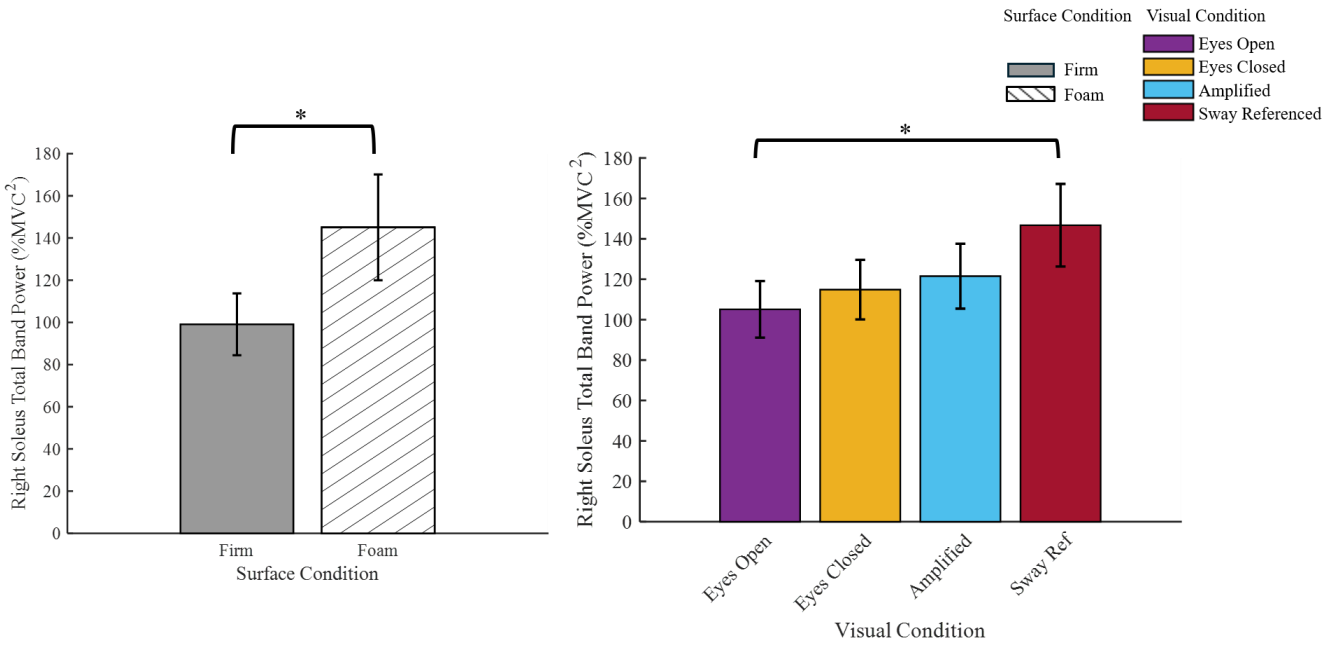

***Figure 6**: Total Band Power of the right soleus. (Left) Displays the main effect of surface. Grey filled bar represents collapsed firm conditions and the hatched bar represents collapsed foam conditions. (Right) Displays the main effect of vision. Colours represent collapsed visual conditions as indicated in the legend. Standard error bars are displayed for both. Significance is indicated between sensory conditions. (*p<0.005, **p<0.001).*

3.4 Relative Frequency Composition

The largest frequency composition was in the ultra-low and low frequency bands, accounting for approximately 90% of frequency composition for all dependent measures. The relative frequency composition of the AP COP and AP COM followed a similar pattern, which displayed that the frequency composition within each frequency band was context-dependent. This context-dependent relationship was evidenced by an increased frequency composition in the medium and high frequency bands for EC, AMP, and SR visual conditions on the foam surface. Further, the right soleus relative frequency composition identified that surface influences muscle activity across all four frequency bands.

3.4.1 Kinetics

3.4.1.1 Ultra-Low Frequency (0-0.1Hz)

The composition analysis of the ultra-low frequency band (0-0.1Hz) for AP COP showed a main effect of surface ($F(1,31)=32.921$, $p<0.001$, $\eta^2=0.515$) and a main effect of vision ($F(3,93)=16.574$, $p<0.001$, $\eta^2=0.348$). There was no significant interaction effect between surface and vision in the ultra-low frequency band for AP COP ($F(3,93)=1.306$, $p=0.277$, $\eta^2=0.040$). Figure 7 shows the significant main effects of surface and vision.

The main effect of surface revealed a decrease in the ultra-low frequency band for the foam surface compared to the firm surface (Figure 7, left). For the main effect of vision, pairwise comparisons confirmed a significant difference between EO and EC ($p<0.001$), EO and SR ($p=0.005$), EC and AMP ($p<0.001$), and SR and AMP ($p<0.001$). EC and SR visual conditions had a lower ultra-low band power composition compared to EO and AMP visual conditions. There was no significant effect of vision between EO and AMP, as well as between EC and SR.

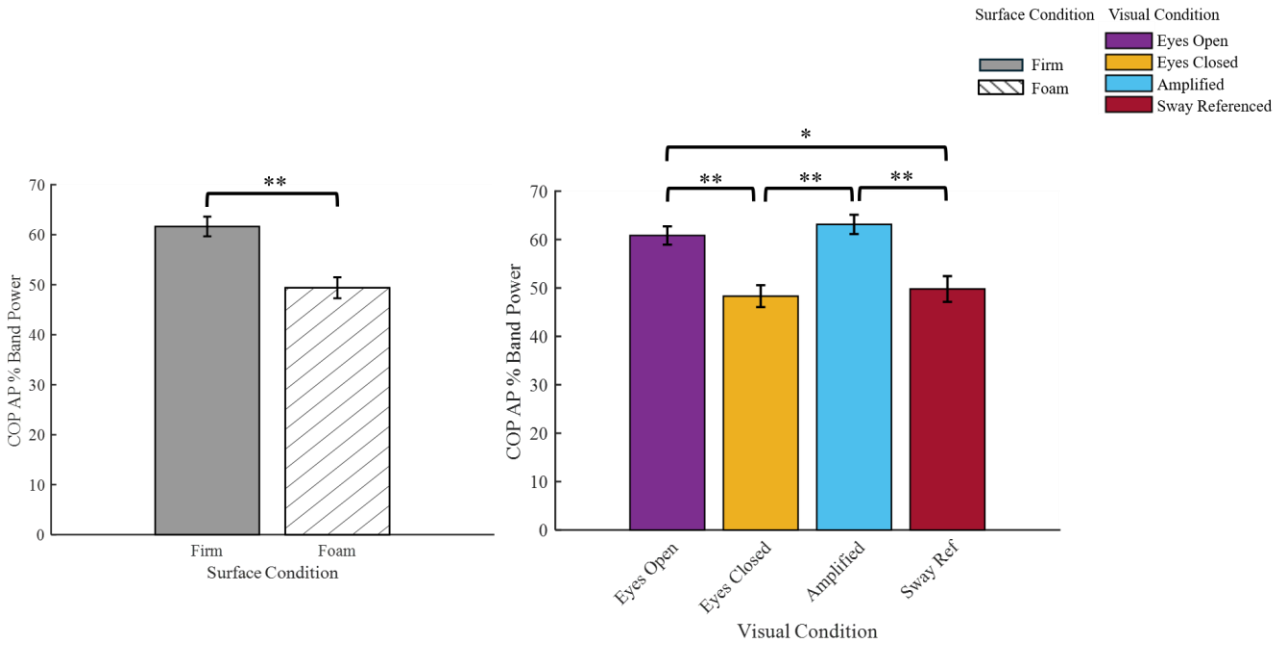

Figure 7*: Relative frequency composition of AP COP for the ultra-low frequency band (0-0.1Hz). (Left) Displays the main effect of surface. Grey filled bar represents collapsed firm conditions and the hatched bar represents collapsed foam conditions. (Right) Displays the main effect of vision. Colours represent collapsed visual conditions as indicated in the legend. Standard error bars are displayed. Significance is indicated between sensory conditions. (*p<0.005, **p<0.001).*

3.4.1.2 Low Frequency Composition (0.1-0.5Hz)

The composition of the low frequency band (0.1-0.5Hz) for AP COP showed a main effect of surface ($F(1,31)=6.726$, $p=0.014$, $\eta^2=0.178$) and a main effect of vision ($F(3,93)=25.072$, $p<0.001$, $\eta^2=0.457$). There was no significant interaction effect between surface and vision in the low frequency band for AP COP ($F(3,93)=0.347$, $p=0.791$, $\eta^2=1.041$). Figure 8 shows the significant main effects of surface and vision.

The main effect of surface revealed an increase in the low frequency band for the foam surface compared to the firm surface (Figure 8, left). For the main effect of vision, pairwise comparisons confirmed a significant difference between EO and AMP ($p<0.001$), EO and SR

(p=0.047), EC and AMP (p<0.001), and SR and AMP (p<0.001). The AMP visual condition had a decreased low frequency band power composition compared to the other visual conditions (EO, EC, and SR). The SR visual condition had an increased low frequency band power composition compared to EO and AMP visual conditions. There was no significant difference between EO and EC visual conditions; however, it approached significance (p=0.054). There was also no significant effect of vision between EC and SR visual conditions.

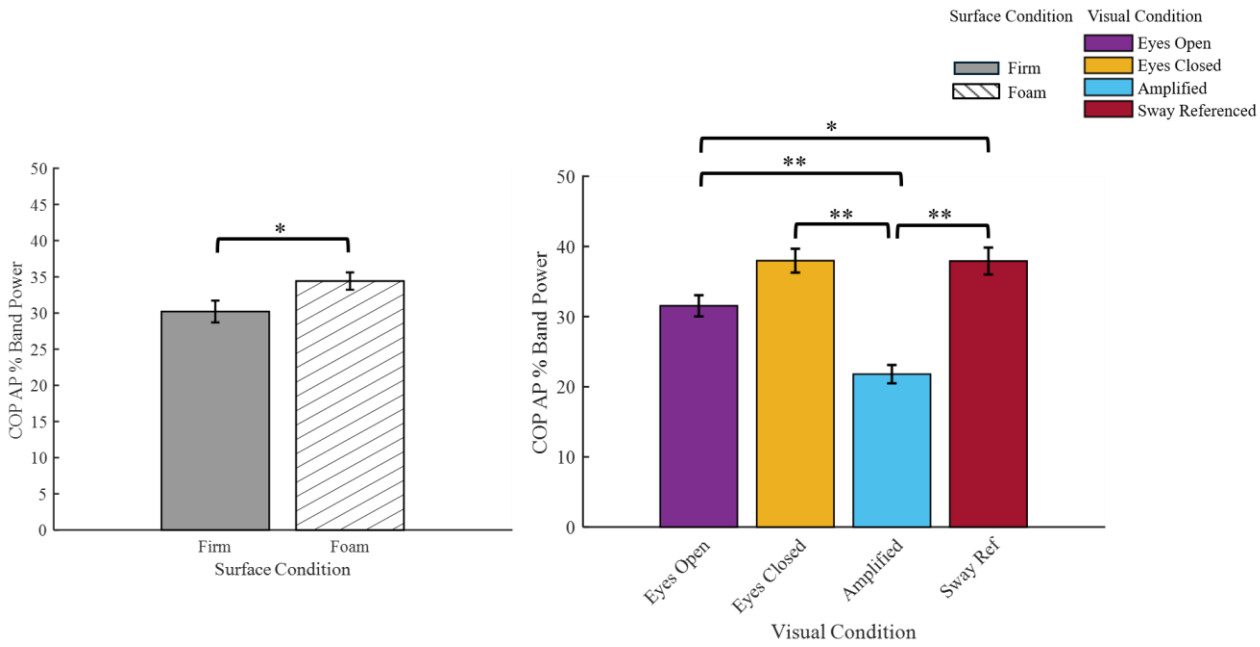

Figure 8: *Relative frequency composition of AP COP for the low frequency band (0.1-0.5Hz). (Left) Displays the main effect of surface. Grey filled bar represents collapsed firm conditions and the hatched bar represents collapsed foam conditions. (Right) Displays the main effect of vision. Colours represent collapsed visual conditions as indicated in the legend. Standard error bars are displayed. Significance is indicated between sensory conditions. (*p<0.005, **p<0.001).*

3.4.1.3 Medium Frequency (0.5-1Hz)

The composition of the medium frequency band (0.5-1Hz) for AP COP showed a main effect of surface ($F(1,31)=40.488$, $p<0.001$, $\eta^2=0.566$) and a main effect of vision

($F(3,93)=19.762$, $p<0.001$, $\eta^2=0.389$). This analysis identified a significant interaction effect between surface and vision in the medium frequency band for AP COP ($F(3,93)=4.835$, $p=0.004$, $\eta^2=0.135$). Figure 9 shows the significant pairwise comparisons between the 8 conditions for the total band power of the AP COP in the medium frequency band.

Post-hoc tests identified significant pairwise comparisons between C3 (AMP) and C4 (SR) on the firm surface. Medium frequency band composition increased for C3 compared to C4 ($p=0.018$). For the firm surface conditions, there were trends towards significance for C1 (EO) and C3 (AMP) ($p=0.078$), and for C2 (EC) and C4 (SR) ($p=0.068$).

On the foam surface, C5 (EO on Foam) was significantly different than C6 (EC on Foam), C7 (AMP on Foam), and C8 (SR on Foam) (all $p<0.001$). In this case, C5 had a lower medium frequency band composition compared to C6, C7, and C8. For the foam surface, there was also a trend towards significance between C7 (AMP on Foam) and C8 (SR on Foam) ($p=0.084$). There were no other significant pairwise comparisons identified.

Pairwise comparisons between firm and foam surfaces for the same visual conditions identified differences between C2 to C6, C3 to C7, and C4 to C8. The firm surface conditions (C2, C3 and C4) had a decreased medium frequency band composition compared to the matched visual condition on the foam surface (C6, C7, and C8) (all $p < 0.001$). There was no significant difference between C1 and C5 ($p=0.160$).

The main effect of surface revealed an increase in the medium frequency band for the foam surface compared to the firm surface. For the main effect of vision, pairwise comparisons confirmed a significant difference between EO and EC ($p<0.001$), EO and AMP ($p<0.001$), EO and SR ($p=0.014$), and SR and AMP ($p<0.001$). EC, AMP, and SR visual conditions had an

increased medium frequency band composition compared to the EO visual condition. The AMP visual condition also displayed an increased medium frequency band power compared to the SR visual condition. There was no significant difference between EC and AMP (p=0.463) and EC and SR (p=0.463) visual conditions.

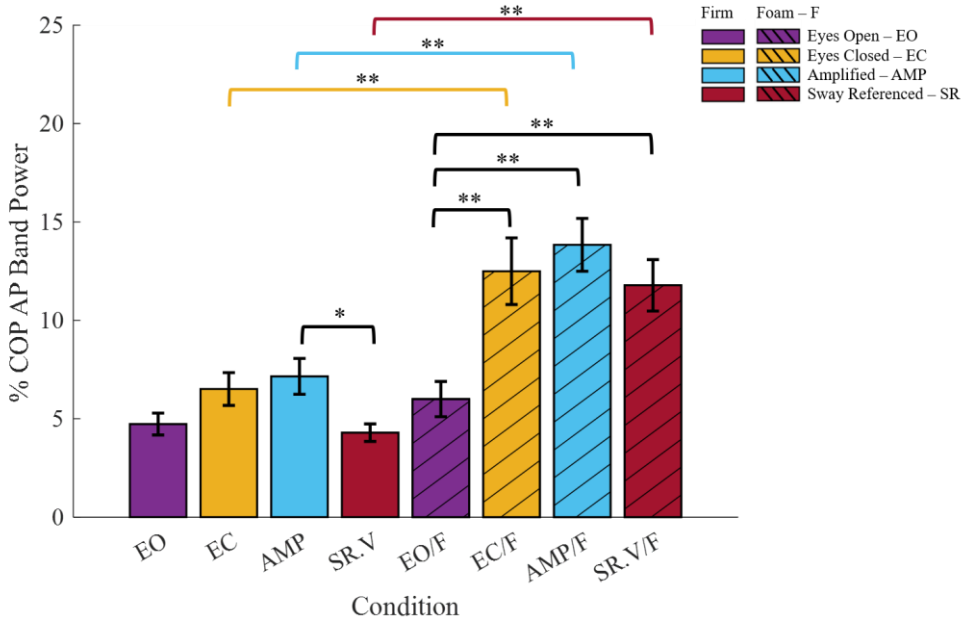

Figure 9: *Relative frequency composition of AP COP for the medium frequency band (0.5-1Hz). Solid bars are firm surface conditions. Hatched bars are foam surface conditions. Colours represent visual conditions as indicated in the legend. Standard error bars are displayed. Significance is indicated between sensory conditions. (*p<0.005, **p<0.001).*

3.4.1.4 High Frequency (1-5Hz)

The composition of the high frequency band (1-5Hz) for AP COP showed a main effect of surface ($F(1,31)=24.375$, $p<0.001$, $\eta^2=0.440$) and a main effect of vision ($F(3,93)=16.801$, $p<0.001$, $\eta^2=0.351$). This analysis also found a significant interaction effect between surface and vision in the high frequency band for AP COP ($F(3,93)=7.284$, $p<0.001$, $\eta^2=0.190$). Figure 10

shows the significant pairwise comparisons between the 8 conditions for the total band power of the AP COP in the high frequency band.

Post-hoc tests identified significant differences between C5 (EO on Foam) compared to C6 (EC on Foam), C7 (AMP on Foam), and C8 (SR on Foam) (all $p<0.001$). C5 had a lower high frequency band composition compared to C6, C7, and C8. Pairwise comparisons between firm and foam surfaces identified significant increases from C2 to C6 ($p=0.003$), C3 to C7 ($p<0.001$), and C4 to C8 ($p<0.001$). The firm surface conditions (C2, C3 and C4) had a decreased medium frequency band composition compared to the matched visual condition on the foam surface (C6, C7, and C8). There was no significant difference between C1 and C5 ($p=0.160$). There was no significant difference between C1 and C5, and there was no significant difference between visual conditions on the firm surface in the high frequency band.

The main effect of surface revealed an increase in the high frequency band for the foam surface compared to the firm surface. For the main effect of vision, pairwise comparisons confirmed a significant difference between EO and EC ($p<0.001$), EO and AMP ($p<0.001$), and EO and SR ($p<0.001$). EC, AMP, and SR visual conditions had an increased medium frequency band composition compared to the EO visual condition. No other significant pairwise comparisons were identified.

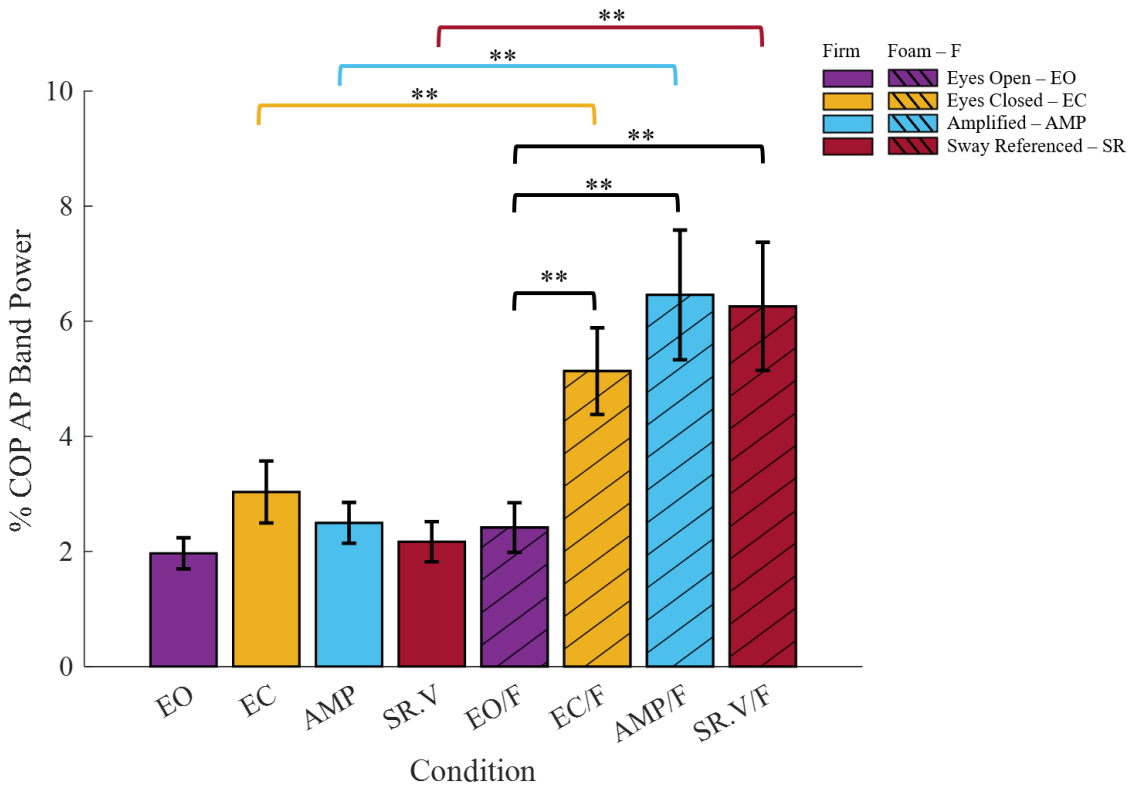

Figure 10: *Relative frequency composition of AP COM for the high frequency band (1-5Hz). Solid bars are firm surface conditions. Hatched bars are foam surface conditions. Colours represent visual conditions as indicated in the legend. Standard error bars are displayed. Significance is indicated between sensory conditions. (*p<0.005, **p<0.001).*

3.4.2 Kinematics

3.4.2.1 Ultra-Low Frequency (0-0.1Hz)

The composition of the ultra-low frequency band (0-0.1Hz) for AP COM showed a main effect of surface ($F(1,31)=17.583$, $p<0.001$, $\eta^2=0.362$) and a main effect of vision ($F(3,93)=21.915$, $p<0.001$, $\eta^2=0.414$). There was no significant interaction effect between surface and vision in the ultra-low frequency band for AP COP ($F(3,93)=34.872$, $p=0.854$, $\eta^2=0.008$). Figure 11 shows the significant main effects of surface and vision for AP COM in the ultra-low frequency band.

The main effect of surface revealed a decrease in the ultra-low frequency band for the foam surface compared to the firm surface. For the main effect of vision, pairwise comparisons confirmed a significant difference between EO and EC ($p=0.012$), EO and AMP ($p=0.003$), EO and SR ($p=0.016$), EC and AMP ($p<0.001$), and SR and AMP ($p<0.001$). EC and SR visual conditions had a lower ultra-low band power composition compared to EO and AMP visual conditions. The AMP visual condition displayed a lower ultra-low frequency band composition compared to the EO visual condition. This pairwise comparison was not identified for AP COP. There was no significant difference between EC and SR.

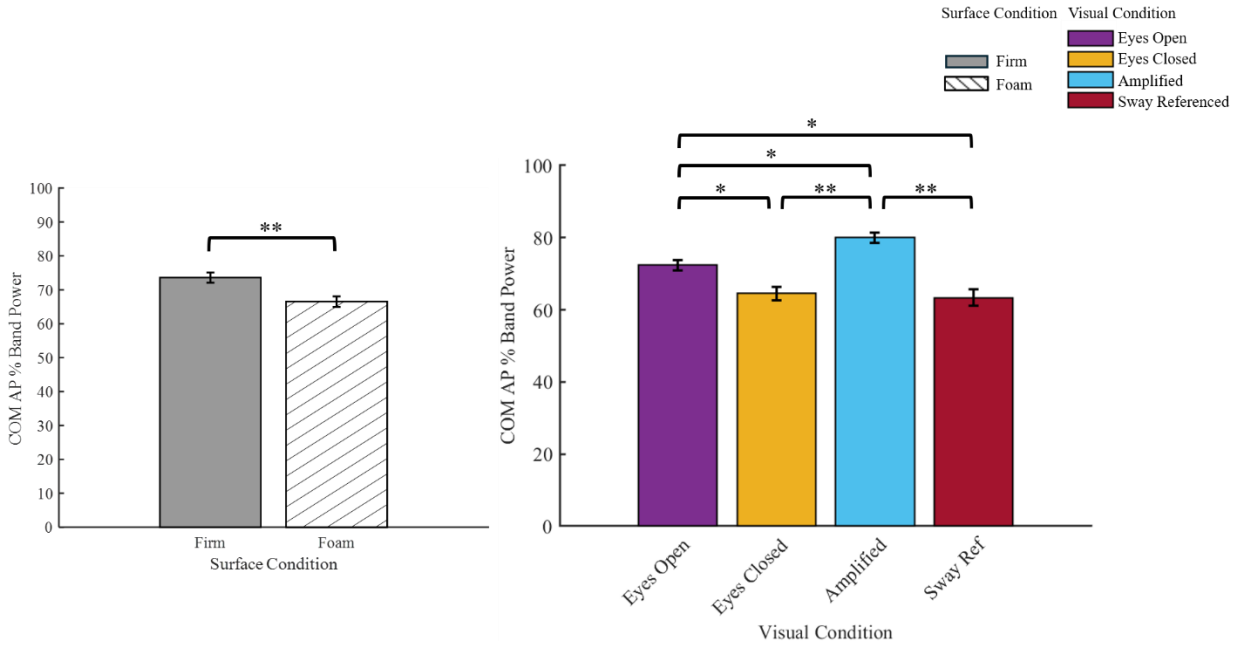

Figure 11: *Relative frequency composition of AP COM for the ultra-low frequency band (0-0.1Hz). (Left) Displays the main effect of surface. Grey filled bar represents collapsed firm conditions and the hatched bar represents collapsed foam conditions. (Right) Displays the main effect of vision. Colours represent collapsed visual conditions as indicated in the legend. Standard error bars are displayed. Significance is indicated between sensory conditions. (*p<0.005, **p<0.001).*

3.4.2.2 Low Frequency (0.1-0.5Hz)

The composition of the low frequency band (0.1-0.5Hz) for AP COM showed a main effect of surface ($F(1,31)=12.349$, $p=0.001$, $\eta^2=0.285$) and a main effect of vision ($F(3,93)=23.206$, $p<0.001$, $\eta^2=0.428$). There was no significant interaction effect between surface and vision in the low frequency band for AP COP ($F(3,93)=0.099$, $p=0.961$, $\eta^2=0.003$). Figure 12 shows the significant main effects of surface and vision for AP COM in the low frequency band.

The main effect of surface revealed an increase in the low frequency band composition for the foam surface compared to the firm surface. For the main effect of vision, pairwise comparisons confirmed a significant difference between EO and EC ($p=0.026$), EO and AMP ($p<0.001$), EO and SR ($p=0.020$), EC and AMP ($p<0.001$), and SR and AMP ($p<0.001$). EC and SR visual conditions displayed an increase in low frequency band composition compared to EO and AMP visual conditions. Further, the AMP visual condition displayed a decreased low frequency band composition compared to the EO visual condition. There was no significant difference between EC and SR.

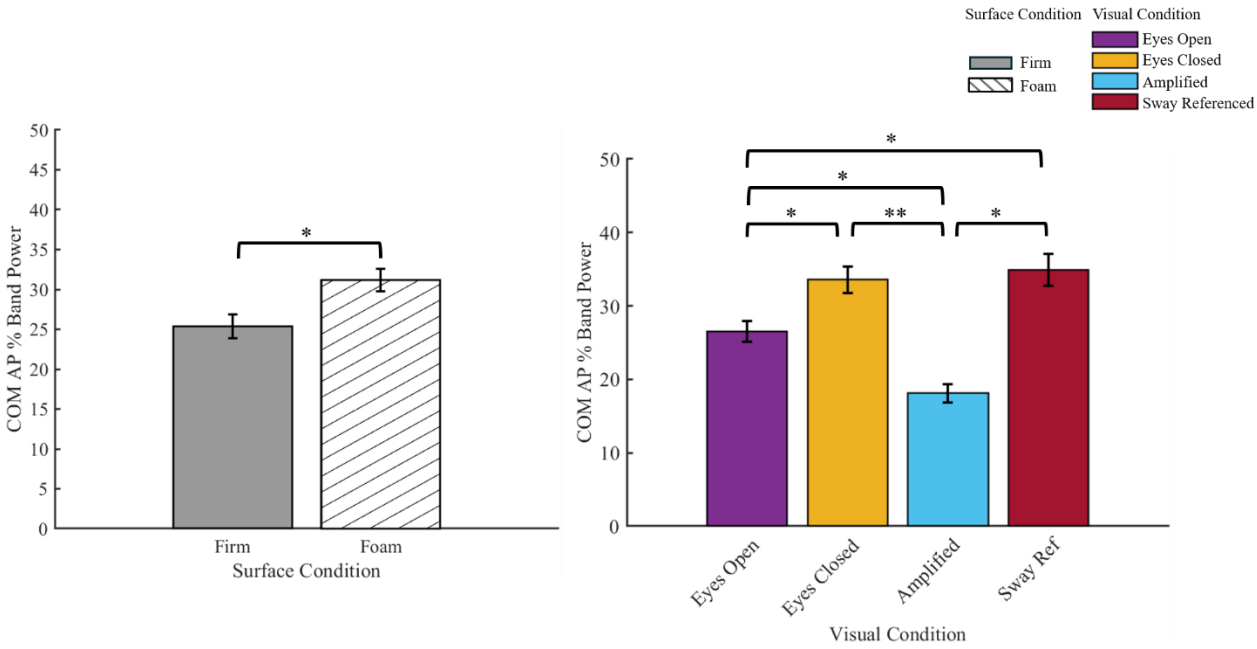

Figure 12: *Relative frequency composition of AP COM for the low frequency band (0.1-0.5Hz). (Left) Displays the main effect of surface. Grey filled bar represents collapsed firm conditions and the hatched bar represents collapsed foam conditions. (Right) Displays the main effect of vision. Colours represent collapsed visual conditions as indicated in the legend. Standard error bars are displayed. Significance is indicated between sensory conditions. (*p<0.005, **p<0.001).*

3.4.2.3 Medium Frequency (0.5-1Hz)

The composition of the medium frequency band (0.5-1Hz) for AP COM showed a main effect of surface ($F(1,31)=44.788$, $p<0.001$, $\eta^2=0.591$) and a main effect of vision ($F(3,93)=12.231$, $p<0.001$, $\eta^2=0.283$). This analysis also found a significant interaction effect between surface and vision in the medium frequency band for AP COM ($F(3,93)=4.211$, $p=0.008$, $\eta^2=0.120$). Figure 13 shows the significant pairwise comparisons between the 8 conditions for the total band power of the AP COM in the medium frequency band.

Post-hoc pairwise comparisons identified differences on the foam surface between C5 (EO on Foam) and the other three visual conditions: C6 (EC on Foam) ($p<0.001$), C7 (AMP on

Foam) ($p<0.001$), and C8 (SR on Foam) ($p=0.002$). C5 had a lower medium frequency band composition compared to C6, C7, and C8. Pairwise comparisons between firm and foam surfaces identified significant increases in medium frequency band composition from C2 to C6, C3 to C7, and C4 to C8 (all $p < 0.001$). The firm surface conditions (C2, C3 and C4) had a decreased medium frequency band composition compared to the matched visual condition on the foam surface (C6, C7, and C8). There was no significant difference between C1 and C5 and there were no significant differences between visual conditions on the firm surface in the medium frequency band for the AP COM.

The main effect of surface revealed an increase in the medium frequency band composition for the foam surface compared to the firm surface. For the main effect of vision, pairwise comparisons confirmed a significant difference between EO and EC ($p=0.002$), EO and AMP ($p<0.001$), and EO and SR ($p=0.044$). The EO visual condition had a lower medium frequency band composition compared to EC, AMP and SR visual conditions. There was no significant increase in medium frequency band composition between AMP and SR visual conditions; however, it approached significance ($p=0.063$). There were no other significant pairwise comparisons in the medium frequency band for the AP COM.

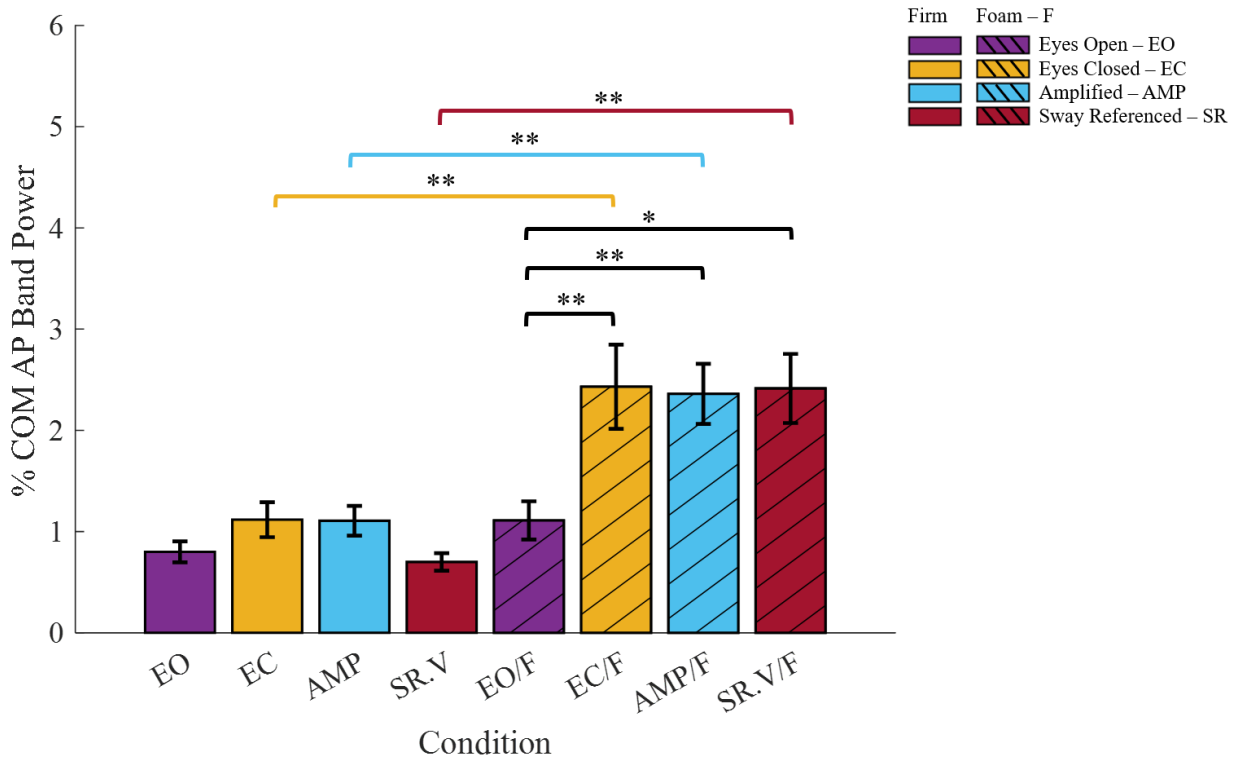

Figure 13: *Relative frequency composition of AP COM for the medium frequency band (0.5-1Hz). Solid bars are firm surface conditions. Hatched bars are foam surface conditions. Colours represent visual conditions as indicated in the legend. Standard error bars are displayed. Significance is indicated between sensory conditions. (*p<0.005, **p<0.001).*

3.4.2.4 High Frequency (1-5Hz)

The composition of the high frequency band (1-5Hz) for AP COM showed a main effect of surface ($F(1,31)=16.678$, $p<0.001$, $\eta^2=0.350$) and a main effect of vision ($F(3,93)=10.218$ $p<0.001$, $\eta^2=0.248$). This analysis also found a significant interaction effect between surface and vision in the high frequency band for AP COM ($F(3,93)=8.297$, $p<0.001$, $\eta^2=0.211$). Figure 14 shows the significant pairwise comparisons between the 8 conditions for the total band power of the AP COM in the high frequency band.

Post-hoc pairwise comparisons identified differences on the foam surface between C5 (EO on Foam) and the other three visual conditions: C6 (EC on Foam), C7 (AMP on Foam), and C8 (SR on Foam) (all $p<0.001$). C5 had a lower high frequency band composition compared to C6, C7, and C8. Pairwise comparisons between firm and foam surfaces for the same visual condition identified significant differences between C2 and C6 ($p=0.002$), C3 and C7 ($p<0.001$), and C4 and C8 ($p<0.001$). The firm surface conditions (C2, C3 and C4) had a decreased high frequency band composition compared to the matched visual condition on the foam surface (C6, C7, and C8). There was no significant difference between C1 and C5, and there were no significant differences between visual conditions on the firm surface in the high frequency band for the AP COM.

The main effect of surface revealed an increase in the high frequency band composition for the foam surface compared to the firm surface. For the main effect of vision, pairwise comparisons confirmed a significant difference between EO and EC ($p<0.001$), EO and AMP ($p<0.001$), and EO and SR ($p=0.008$). The EO visual condition had a lower high frequency band composition compared to EC, AMP and SR visual conditions. There were no other significant pairwise comparisons in the medium frequency band for the AP COM.

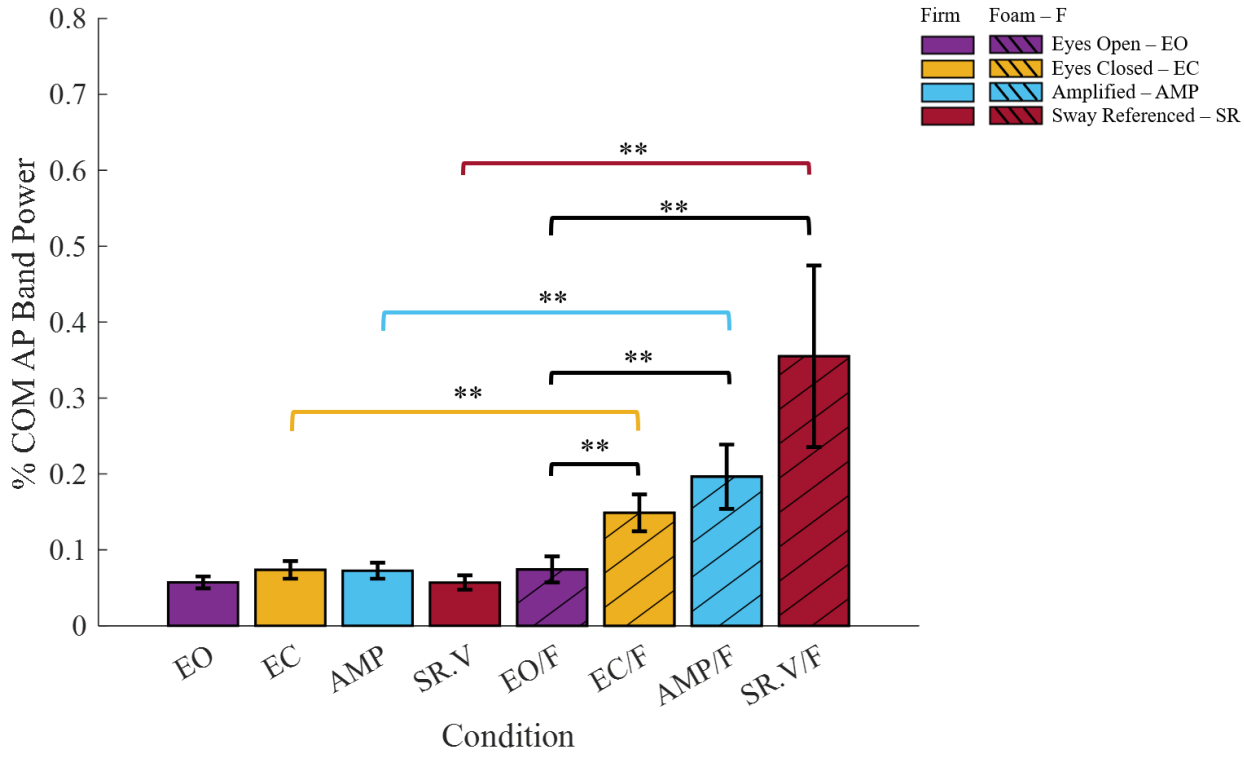

Figure 14: *Relative frequency composition of AP COM for the high frequency band (1-5Hz). Solid bars are firm surface conditions. Hatched bars are foam surface conditions. Colours represent visual conditions as indicated in the legend. Standard error bars are displayed. Significance is indicated between sensory conditions. (*p<0.005, **p<0.001).*

3.4.3 EMG

3.4.3.1 Ultra-Low Frequency (0-0.1Hz)

The composition of the ultra-low frequency band (0-0.1Hz) for the right soleus showed a main effect of surface ($F(1,29)=11.041$, $p=0.002$, $\eta^2=0.276$). The main effect of surface revealed a decrease in the ultra-low frequency band composition for the foam surface compared to the firm surface (Figure 15). There was no main effect of vision for the right soleus in the ultra-low frequency band ($F(3,87)=2.072$, $p=0.110$, $\eta^2=0.067$). This analysis did not identify a significant interaction between surface and vision; however, it approached significance ($F(3,87)=2.521$,

p=0.063, η^2=0.080). Figure 15 shows the main effect of surface of the ultra-low frequency band composition for the right soleus.

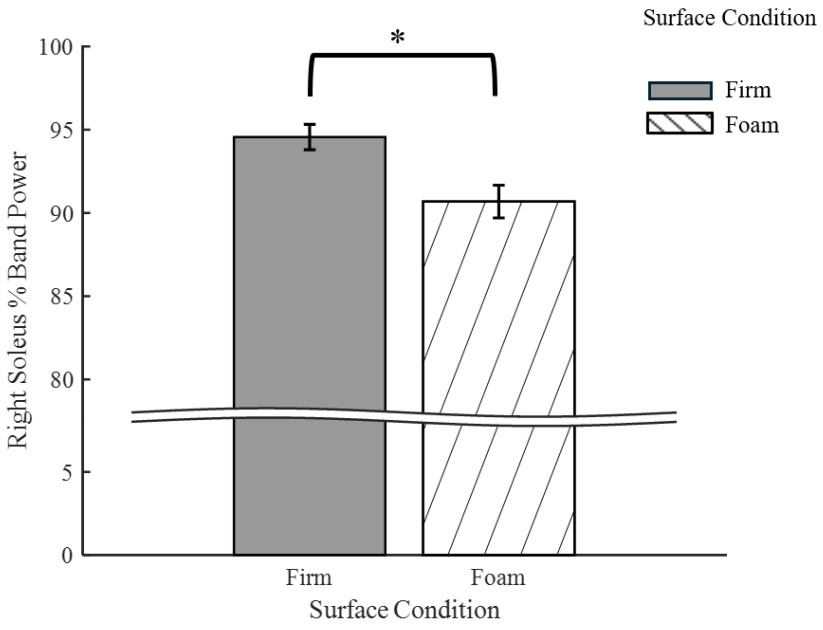

Figure 15: *Relative frequency composition of the Right Soleus for the ultra-low frequency band (0-0.1Hz). The solid bar represents the firm surface conditions, and the hatched bar represents the foam surface conditions. Significance is indicated between sensory conditions. (*p<0.005, **p<0.001).*

3.4.3.2 Low Frequency (0.1-0.5Hz)

The composition of the low frequency band (0.1-0.5Hz) for the right soleus showed a main effect of surface ($F(1,29)=27.055$, $p<0.001$, $\eta^2=0.483$) and a main effect of vision ($F(3,87)=15.154$, $p<0.001$, $\eta^2=0.343$). This analysis also identified a significant interaction effect between surface and vision in the low frequency band for the right soleus ($F(3,87)=4.267$, $p=0.007$, $\eta^2=0.128$). Figure 16 shows the significant pairwise comparisons between the 8 conditions for the total band power of the right soleus in the low frequency band.

Post-hoc tests identified significant pairwise comparisons on the foam surface between C7 (AMP on Foam) and C5 (EO on Foam), C6 (EC on Foam), and C8 (SR on Foam) (all $p<0.001$). C7 had a decreased low frequency band composition compared to C5, C6, and C8. Pairwise comparisons between firm and foam surfaces for the same visual condition identified significant differences between C1 to C5, C2 to C6, and C4 to C8 (all $p<0.001$). The firm surface conditions (C2, C3 and C4) had a decreased high frequency band composition compared to the matched visual condition on the foam surface (C6, C7, and C8). There was no significant difference between C3 and C7; however, it approached significance ($p=0.090$). There were no significant differences identified for visual conditions on the firm surface.

The main effect of surface revealed an increase in the low frequency band composition for the foam surface compared to the firm surface. For the main effect of vision, pairwise comparisons confirmed a significant difference between the AMP vision condition and the other visual conditions (EO, EC, and SR) (all $p<0.001$). EO, EC, and SR visual conditions had an increased low frequency band composition compared to the AMP visual condition. There were no significant differences between EO, EC, and SR visual conditions.

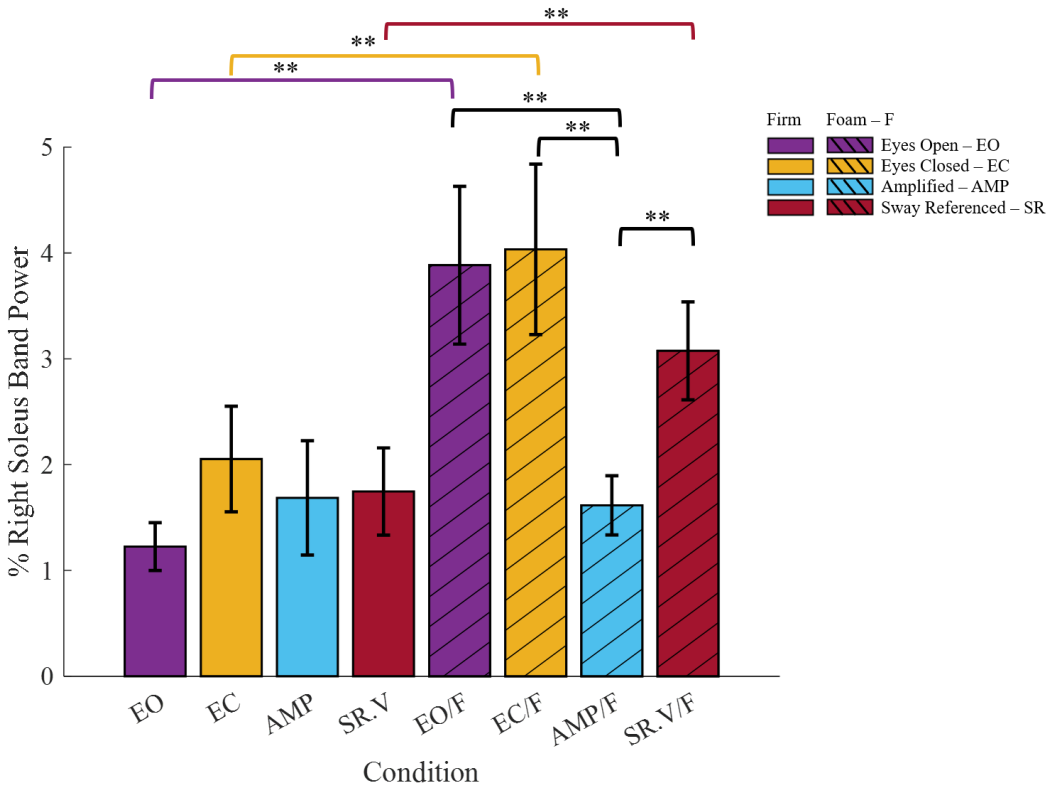

Figure 16: *Relative frequency composition of the Right Soleus for the low frequency band (0.1-0.5Hz). Solid bars are firm surface conditions. Hatched bars are foam surface conditions. Colours represent visual conditions as indicated in the legend. Standard error bars are displayed. Significance is indicated between sensory conditions. (*p<0.005, **p<0.001).*

3.4.3.3 Medium Frequency (0.5-1Hz)

The composition of the medium frequency band (0.1-0.5Hz) for the right soleus showed a main effect of surface ($F(1,29)=28.611$, $p<0.001$, $\eta^2=0.497$) and a main effect of vision ($F(3,87)=3.627$, $p=0.016$, $\eta^2=0.111$). There was no significant interaction effect between surface and vision for the right soleus in the medium frequency band ($F(3,87)=0.524$, $p=0.667$, $\eta^2=0.018$). Figure 17 shows the significant main effects of surface and vision for the right soleus in the ultra-low frequency band.

The main effect of surface revealed an increase in the medium frequency band composition for the foam surface compared to the firm surface. For the main effect of vision, pairwise comparisons confirmed a significant difference between EO and EC (p=0.004). The EC visual condition displayed an increased medium frequency band composition compared to the EO visual condition. There were no other significant pairwise comparisons in the medium frequency band.

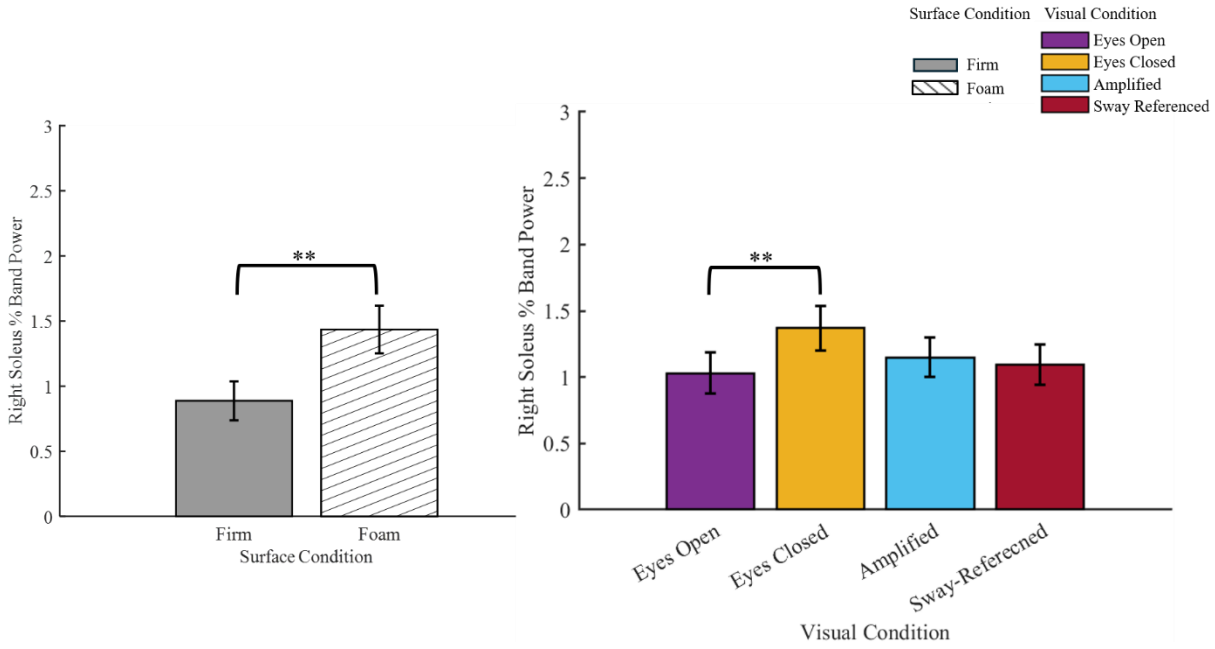

Figure 17: *Relative frequency composition of the right soleus for the medium frequency band (0.5-1Hz). (Left) Displays the main effect of surface. Grey filled bar represents collapsed firm conditions and the hatched bar represents collapsed foam conditions. (Right) Displays the main effect of vision. Colours represent collapsed visual conditions as indicated in the legend. Standard error bars are displayed. Significance is indicated between sensory conditions. (*p<0.005, **p<0.001).*

3.4.3.4 High Frequency (1-5Hz)

The composition of the high frequency band (1-5Hz) for the right soleus showed a main effect of surface ($F(1,29)=61.029$, $p<0.001$, $\eta^2=0.678$) and a main effect of vision ($F(3,87)=5.321$, $p=0.002$, $\eta^2=0.155$). There was no significant interaction effect between surface and vision for the right soleus in the high frequency band ($F(3,87)=1.068$, $p=0.367$, $\eta^2=0.036$). Figure 18 shows the significant main effects of surface and vision for the right soleus in the high frequency band.

The main effect of surface revealed an increase in the high frequency band composition for the foam surface compared to the firm surface. For the main effect of vision, pairwise comparisons confirmed a significant difference between EO and EC ($p<0.001$). The EC visual condition displayed an increased high frequency band composition compared to the EO visual condition. EC and AMP visual conditions approached significance ($p=0.060$). There were no other significant pairwise comparisons in the high frequency band. Table 3 summarizes the results for all variables and dependent measures (Section 3.2).

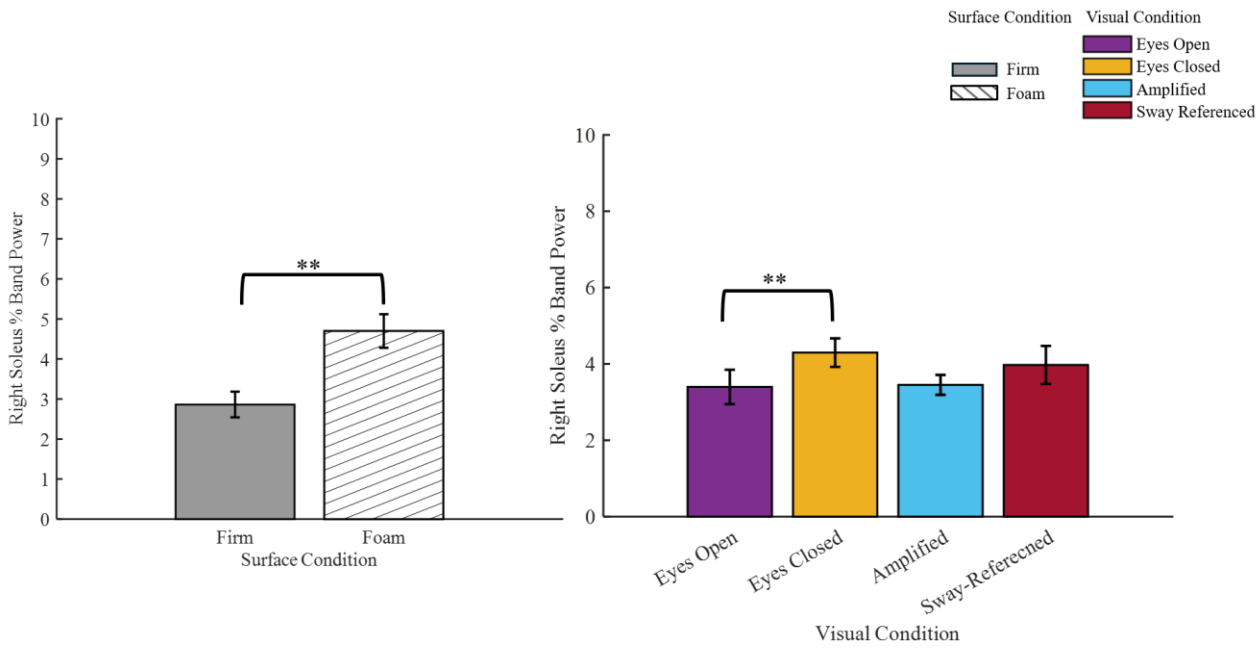

Figure 18: *Relative frequency composition of the right soleus for the high frequency band (1-5Hz). (Left) Displays the main effect of surface. Grey filled bar represents collapsed firm conditions and the hatched bar represents collapsed foam conditions. (Right) Displays the main effect of vision. Colours represent collapsed visual conditions as indicated in the legend. Standard error bars are displayed. Significance is indicated between sensory conditions. (*p<0.005, **p<0.001).*

Chapter 4: Discussion

The purpose of this thesis was to critically examine and challenge the FSCF to improve characterization of how sensory information shapes and regulates standing balance control. The results of this thesis suggest that the FSCF may not be a comprehensive model to describe the sensory contributions to upright stance. This was primarily evidenced by contributions of the somatosensory and visual systems outside of the FSCF-hypothesized frequency bands. Specifically, somatosensory information showed contributions beyond the high frequency band (1-5Hz) to lower frequency bands, evidenced by the decreased composition of the ultra-low frequency band for the foam surface conditions. Further, visual information showed contributions beyond the ultra-low frequency band (0-0.1Hz), evidenced by increased frequency composition with AMP visual information in the medium and high frequency bands.

The results overall supported hypothesis 1, that total band power would change in a context-dependent manner in response to altered sensory information, as evidenced by significant differences in total band power between sensory conditions. This outcome aligned with work that showed that removed or unreliable sensory information increased total band power [64,76]. For example, the EO, EC, and SR visual conditions on the foam surface displayed increased total band power compared to other visual conditions on the foam surface, congruent with previous work [10,64]. However, this increase did not occur for the AMP visual condition, which showed a reduction in total band power for the AP COP and AP COM. This suggests that the AMP visual condition may compensate for the effect of foam. This finding contrasts with the FSCF, which does not hypothesize overlap between the visual and somatosensory related frequency bands.

The current FSCF is based on relative frequency band composition to define visual (0-0.1Hz), vestibular (0.1-0.5Hz), cerebellar (0.5-1Hz), and somatosensory (1-5Hz) contributions to upright stance [32]. For this thesis, the analysis of relative frequency band composition indicated that depending on the sensory information available, frequency composition across variables shifted. Specifically, when both vision and somatosensory information were altered during EC, AMP, and SR on foam, there was a shift towards higher composition of frequency power in the medium and high frequency bands (>0.5Hz). The composition of the frequency signal did not follow the defined frequency bands of the FSCF, as somatosensory information contributed to frequencies lower than the high frequency band (1-5Hz) (Figure 7) and visual information contributed to frequencies higher than the ultra-low frequency band (0-0.1Hz) (Figure 9 & 10). The shifts in frequency composition extending beyond the proposed frequency bands of the FSCF support hypothesis 2, that somatosensory and visual information will extend beyond the FSCF-hypothesized frequency bands, and that there is a disproportionate shift of frequency composition when two sensory systems are manipulated.

The results of this thesis provide evidence that relating sensory contributions to upright stance to specific frequency bands does not fully describe the full extent of how sensory systems interact with each other to successfully maintain upright stance. It is important to accurately describe the frequency-specific sensory contributions to upright stance, as it provides a basis for balance data to be interpreted in relation to the temporal characteristics of postural control, ranging from slower sway regulation to faster corrective responses. Thus, the direct interpretations provided by the FSCF do not fully describe the sensory contributions to balance, as it fails to describe how sensory systems can operate below or beyond their hypothesized frequency bands.

4.1 Total Band Power

4.1.1 Kinetics

On the firm surface, there was no significant difference between visual conditions (EO, EC, AMP, and SR) for the total band power of the AP COP. The lack of significance between visual conditions on the firm surface suggests that the process of sensory reweighting can maintain frequency power similar to the EO condition when visual information is modified during EC, AMP, and SR conditions. Other work examining the process of sensory reweighting using an SR platform and visual scene has shown that somatosensory and vestibular information can attenuate the effects of unreliable visual information [77]. For these results, the Independent Channel Theory would postulate that a downweighting of vision would upweight vestibular and somatosensory systems [1]. This theory may explain the results of visual conditions on the firm surface for the AP COP total band power, as when visual information was altered or removed, there was no significant difference between conditions. This provided evidence that there was an upweighting of the vestibular and somatosensory systems to maintain total band power of the AP COP.

For the AP COP, all visual conditions on foam (EO, EC, AMP, and SR) displayed an increase in total band power compared to the visually matched firm surface condition. The foam surface impacts the mechanics of upright stance through inputs to joint receptors and cutaneous mechanoreceptors [18], increases the magnitude of feedforward muscle activity [16], and increases torque variability of the ankle plantar and dorsiflexor muscles [15]. Thus, the foam surface both impacts the afferent somatosensory information and subsequent postural control strategies to maintain upright stance. This supports the change of total band power for the AP COP, as total band power increased on the foam surface for all visual conditions.

However, within foam surface conditions, EO, EC, and SR conditions were significantly different from the AMP visual condition. Specifically, the AMP visual condition (C7) had a lower total band power than EO, EC, and SR. This suggests that when somatosensory information is made unreliable with AMP visual information (C7, AMP on Foam), AMP visual information may compensate for the increase in frequency power introduced by the foam surface. The prioritization of visual information has been found when investigating the process of sensory reweighting, which identified that there was a preference to shift from high to low amplitude strategies [2]. Furthermore, previous work that investigated AMP OF has identified that AMP visual information reduced sway amplitude [26]. The effect of the AMP visual condition did not appear on the firm surface, supporting the interpretation of increased visual weighting when both vision and somatosensation are altered. This finding suggests that when somatosensory and vestibular information were fully available, the processes of sensory reweighting can maintain the same levels of AP COP total band power as when visual information is altered. On a foam surface, AMP visual information decreased total band power compared to other visual conditions (EO, EC, and SR), which can be explained by the process of sensory reweighting, such that low amplitude afferent visual information is prioritized to maintain balance. All together, these outcomes suggest that the process of sensory reweighting is context-dependent and will shift prioritization of balance relevant information to maintain upright stance based on available and reliable sensory information.

4.1.2 Kinematics

The results of the total band power for the AP COM were similar to AP COP except for the AMP visual conditions, which showed no difference between surfaces. The mechanics of upright stance postulate that the COM is corralled by the COP [4,5], such that the COM signal is

related to the COP but contains less amplitude and is generally maintained at a lower frequency [4]. In this work, as the frequency of the COP increases, so did that of the COM, which shows that the COM and COP are related in maintaining upright stance, as the body maintains posture as an inverted pendulum, despite changes in sensory conditions [78].

During AMP visual conditions, there was no significant difference between firm and foam surfaces. However, on the foam surface, the AMP visual condition for the AP COM was significantly different than all other visual conditions. This adaptation of COM control gives evidence that AMP visual information reduces total band power on a foam surface compared to other visual conditions (EO, EC, and SR). In the literature, it has been shown that AMP visual information reduces COP and AP Head Displacement [26], which would suggest that the AP COM should also reduce as the body stands as an inverted pendulum [5,78]. Furthermore, studies investigating motor control strategies when visual and somatosensory information is manipulated suggest that there is a preference to increase muscle activity and joint movement in the lower body compared to the upper body to maintain upright stance [79]. Thus, the adaptation in motor strategies to increase muscle activity and joint movement in the lower body compared to the upper body may explain why the AP COM did not reflect the same changes as the AP COP. The manipulation of both somatosensory and visual information adjusts the motor strategies of the inverted pendulum, reducing the amount of AP COM total band power during AMP vision on foam.

4.1.3 Electromyography

Total band power of the right soleus muscle showed an effect of surface consistent with AP COM and AP COP. The foam surface increased total band power compared to the firm surface. The soleus muscle is responsible for continuous ankle stabilization in the AP direction [80].

Moritani et al., (1991) found that as task difficulty increased, soleus mean EMG amplitude and mean power frequency increased [81]. This evidence supports the increase in total band power between surface conditions in this paradigm, as the foam surface nullifies ankle proprioception and increases the amount of ankle torque variability required to maintain larger changes in postural sway [15].

To investigate the effect of visual conditions on the total band power of right soleus muscle activity, there was a significant difference between EO and SR visual conditions. The SR visual condition required a greater right soleus total band power compared to the EO condition. During the EO visual condition, the visual system receives 1:1 real-world optic flow, while during the SR visual condition, motion cues are removed. Evidence from a SOT showed that visual disruption of either EC or SR increased postural sway [82]. An increased amount of postural sway would also increase the total band power associated with the right soleus muscle, as evident in the results of this thesis. Overall, the total band power of the right soleus muscle was influenced by both surface and vision independently. This suggests that adaptations in total band power for the right soleus were context-dependent such that increases in total band power were not necessary to compensate for all sensory conditions.

4.1.4 Total Band Power Summary

The changes in total band power showed a context-dependent relationship between sensory conditions. This context-dependent relationship supports hypothesis 1 of this thesis and can be explained by prioritization of afferent sensory information during the process of sensory reweighting, and motor strategies influencing the dynamics of the inverted pendulum.

The effect of surface between all the dependent variables is consistent with the literature; when somatosensory information is made unreliable by the foam surface, there is an increase in total band power reflective of changes in sensory reweighting, adaptations in ankle torque variability, and increased feedforward control. The effects of vision differed between the dependent variables, such that total band power did not show identical results between the visual conditions. For example, AMP vision on foam displayed a priority for low amplitude control, evidenced by reducing AP COP and AP COM total band power compared to the other visual conditions on foam (EO, EC, and SR). Despite the reduction in total band power for the AP COP and AP COM, right soleus muscle activity did not reflect the same reduction in total band power during AMP vision. Furthermore, all visual conditions increased total band power between the firm and foam surface for the AP COP; however, for the AP COM, all conditions increased total band power between firm and foam surface except for the AMP visual conditions. The effect of AMP vision on the AP COP and AP COM suggests that there may be a priority for visual information during sensory reweighting, such that there is prioritization for low frequency control when somatosensory information is made unreliable via the foam surface. Further, the right soleus evidenced a change between EO and SR visual conditions, suggesting that when visual information is available but without motion cues, there is an increased reliance on ankle plantar flexors, possibly evidencing an alternative strategy to maintain upright stance which is not identified in the AP COP and AP COM. Overall, the total band power analysis suggests that the absolute frequency power to maintain upright stance has a context-dependent relationship with sensory information and dynamically changes motor strategies to maintain upright stance during sensory conflict.

4.2 Composition of the Frequency Bands

The FSCF postulates that the frequency composition of the AP COP is related to specific sensory systems (Figure 1). It is typically defined with 4 frequency bands: ultra-low (0-0.1Hz), low (0.1-0.5Hz), medium (0.5-1Hz) and high (1-5Hz), representing the visual, vestibular, cerebellar, and somatosensory contribution to balance, respectively. This hypothesized framework is based on the premise that when sensory input is altered, there are specific and relative increases and decreases in frequency composition based on the afferent balance-relevant sensory information. For example, evidence for the contribution of the visual system suggests that when maintaining upright stance with EO versus EC, there is a relative shift from the ultra-low frequency band to the low, medium and high frequency bands, suggesting that the visual contribution to balance is associated with ultra-low frequency (Appendix A & B) [31,33]. The FSCF provides a simple way to interpret frequency data, which relates frequency data to a specific contributory mechanism. However, the FSCF fails to incorporate the overlapping behaviour and contributions of sensory systems, which may oversimplify the sensory contributions to balance and lead to inaccurate interpretations of frequency data during upright stance.

4.2.1 Ultra-Low Frequency Band

The ultra-low frequency band has been postulated to be related to the visual contribution to upright stance between 0-0.1Hz [31,33]. The visual system contributes to balance by providing information about body orientation and self-motion relative to the surrounding environment, allowing the CNS to use external spatial references to maintain postural stability [1,6]. In the literature, vision is related to the ultra-low frequency band based on work investigating visual scene motion and removal of visual information, which produced postural sway between 0.02Hz

and 0.2Hz [31,33,83]. This evidence is the basis of the ultra-low frequency band, and when using the FSCF to interpret visual contributions to upright stance, a 0-0.1Hz frequency range is used.

In the ultra-low frequency band, the FSCF would not predict a compositional change between the firm and the foam surface, as a change in support-surface is not related to a change in visual information. The FSCF would postulate that EC and SR vision would decrease compared to EO, and AMP vision should increase compared to EO (Appendix A & B). The data of this thesis provided evidence that somatosensory information influenced ultra-low frequency composition across all dependent variables (AP COP, AP COM, and right soleus muscle activity), which displayed decreased ultra-low frequency band composition (Figure 7, 11, & 15).

The observed decrease in ultra-low frequency band composition on the foam surface suggests that somatosensory information extends below the high frequency band (1-5Hz). This result is consistent with other work investigating the effects of foam on standing balance, which found that foam surfaces increased torque variance at frequencies above 0.1Hz [15]. The somatosensory system can be involved in ultra-low frequency control through the deformation of musculoskeletal tissue. Further, previous work has suggested that tonic muscle activity is sufficient for maintaining balance passively [46,53,84]. In this study, the right soleus muscle activity decreased frequency composition in the ultra-low frequency band when participants stood on the foam surface. This suggests that there is a shift from tonic, passive control to more active control when standing on foam. A shift from ultra-low to low, medium and high frequency bands represents more ballistic, active activation of the right soleus [85]. The shifts in frequency between surfaces provided evidence that changes in ultra-low frequency composition may not be entirely associated with specific sensory systems but instead are related to the specific task demands and alterations of sensory input.

For the ultra-low frequency band, the FSCF would have predicted that frequency composition would decrease when vision was removed or made unreliable, with EC and SR showing lower values than EO. The results of this thesis support this prediction, as EC and SR visual conditions displayed a decrease in ultra-low frequency band composition compared to the EO and AMP visual conditions for the AP COP and AP COM (Figure 7 & 11). This result may be explained by a downweighting of visual information, which would indicate a need to shift to higher frequency upright stance strategies due to sensory reweighting processes defined by the Independent Channel Theory [1]. This finding is congruent with the evidence that supports the FSCF, which identified a shift from ultra-low frequency to higher frequency bands when vision was removed or altered [31,33]. Further, when assessing the differences between EO and AMP visual conditions, the FSCF would predict an increase in ultra-low frequency composition, which was only identified by the AP COM in this thesis. The AP COP and right soleus muscle activity did not show an increase in ultra-low frequency composition, which would not have been predicted by the FSCF. The effect of AMP visual information has been demonstrated in the literature, showing that when increasing OF, there is an increase in medium and high frequency band power, suggesting that visual information extends beyond the ultra-low frequency band [86]. Furthermore, work investigating visual perturbations has found that visual information can evoke sway up to 2Hz [1], suggesting that visual information may influence upright stance control beyond the ultra-low frequency band (0-0.1Hz).

Overall, the ultra-low frequency band showed mixed results in relation to supporting the FSCF. The FSCF would not have predicted a change in ultra-low frequency band composition between the firm and foam surface, as it is not involved in vision, neglecting the inherent passive and mechanical control of upright stance associated with the somatosensory system. Further, the

AP COP and AP COM showed a decrease in frequency composition in the ultra-low frequency band when comparing EC and SR to EO, congruent with evidence supporting the FSCF. However, AMP vision increased for the AP COM but did not show significance for the AP COP or right soleus, demonstrating that the ultra-low frequency composition is not influenced only by the visual contributions to balance. Taken together, the evidence within the ultra-low frequency band suggests that the FSCF-hypothesized range does not accurately explain visual contributions to upright stance for all dependent variables, primarily neglecting the contribution of the somatosensory system in the ultra-low band.

4.2.2 Low Frequency Band

The low frequency band (0.1-0.5Hz) is related to the vestibular contributions to upright stance [43]. Some of the evidence for the frequency-specific vestibular contributions to upright stance consists of looking at those with vestibular loss, which evidences an increased frequency power between 0.1-1Hz [28,43,76]. This evidence forms the basis for the low frequency band; within the FSCF, vestibular contributions to upright stance are interpreted within the 0.1–0.5 Hz frequency range.

In the low frequency band, the FSCF accurately predicted the significant changes between visual and surface conditions observed in this work (Appendix A & B). The FSCF would predict an increase between firm and foam surfaces, as the downweighting in somatosensory information due to its unreliability on the foam surface would likely lead to an upweighting of vestibular contributions, as proposed by the Independent Channel Theory [1]. The results of this study supported the FSCF in the low frequency band, as surface increased low frequency band composition for all dependent variables (AP COP, AP COM, and right soleus muscle activity). However, right soleus muscle activity did not increase in low frequency band

composition with a change in surface for the AMP visual conditions. In this case, visual information may be prioritized, as evidenced in *section 4.1.* The decrease in right soleus muscle activity in the low frequency band during AMP vision on foam compared to EO, EC, and SR vision provided further evidence that AMP visual information may compensate for the effects of foam.

For the visual conditions, the FSCF would have predicted an increase in low frequency band composition for EC and SR due to unreliable or removed visual information and a decrease in AMP due to the upweighting of visual information. This prediction can be supported by the Independent Channel Theory, as when vision is removed or made unreliable, vestibular information will be upweighted, showing an increase in low frequency band composition [1]. The FSCF predictions are supported by the results of this thesis, as compared to the EO condition, EC (approaching significance for the AP COP) and SR visual conditions increased, and AMP visual conditions decreased compared to EO for the AP COP and AP COM in the low frequency band.

For the results of the AMP visual condition, based on the Independent Channel Theory, visual information in this case was upweighted, downweighting the vestibular contribution, reflecting a decreased low frequency band composition [1]. The decrease in low frequency band composition associated with AMP provides evidence that there was a prioritization of visual information during balance control. However, this prioritization does not negate the contribution of the vestibular system; visual and vestibular systems work together to cohesively generate postural responses. For example, OF is the pattern of visual motion generated on the retina by the relative movement between the observer and the surrounding environment, which can be a result of self-motion or environmental movement [24], which generates corresponding vestibular signals – the two must be integrated to determine if OF is from self or environmental movement [87,88].

Thus, the balance-relevant cues from AMP can be a combination of visual and vestibular processing. Overall, the FSCF predicted changes in low frequency band composition that can be related to the vestibular contributions to balance; however, it does not fully explain how visual or somatosensory inputs to balance control are not related to low frequency band composition.

4.2.3 Medium Frequency Band

The medium frequency band (0.5-1Hz) has been related to the cerebellum's contribution to upright stance [54]. The cerebellum is responsible for error detection, feedforward control, coordination, and sensory integration and includes pathways relevant for processing visual, vestibular, and somatosensory information [34,58,89]. The FSCF relates the medium frequency band to the cerebellum's contribution to upright stance, primarily based on literature investigating cerebellar disorders. In cerebellar ataxia, it was found that there was prominent low frequency sway below 1Hz [54]. This evidence is the basis of the medium frequency band, and when using the FSCF to interpret cerebellar contributions to upright stance, a 0.5-1Hz frequency range is used.

In the medium frequency band, the FSCF would not accurately predict all the observed differences between conditions in the present work. The FSCF would predict that a foam surface would increase the composition of the medium frequency band due to the increased error correction reflected by increased torque variability, and feedforward control needed to maintain upright stance on a foam surface [15,16]. For the AP COP and AP COM, there was an increase in medium frequency band composition between firm and foam surfaces for the EC, AMP, and SR visual conditions, and a main effect of surface was identified for the right soleus. The EC, AMP, and SR conditions increased on foam, which follows the prediction of the FSCF, as when visual and somatosensory information is altered, there is an increased need for the cerebellum's

responsibilities to balance control, including feedforward control, error correction, and integration of sensory information. The EO condition did not show a significant difference between the firm and foam conditions for the AP COP and AP COM in the medium frequency band, suggesting that when visual information is not manipulated, there is no upregulation of the cerebellar contribution to balance, despite unreliable somatosensory information. This is congruent with work that investigated the effects of foam on frequency power and showed no change at frequencies between 0.4-4Hz when standing on a foam surface [90].

On the firm surface, the AP COP displayed a significant difference between AMP and SR visual conditions. The AMP visual condition had a greater medium frequency band composition compared to the SR visual condition on the firm surface. This provided further evidence that the visual contributions to balance extend beyond the ultra-low frequency band. Visual information related to self-motion is directly tied into the visuo-cerebellar pathway where visual motion cues are integrated with vestibular and proprioceptive inputs to maintain spatial orientation [34]. In the present paradigm, the AMP visual condition increases the amount OF, which in turn increases the perception of self-motion [25]. This may result in increased integration between the sensory systems and a higher rate of error detection, which are processes of the cerebellum resulting in increased medium frequency band composition. On the other hand, the SR visual condition removes motion cues from the environment, making visual information unreliable. On the firm surface, sensory reweighting processes can upweight somatosensory and vestibular information, reducing the amount of high frequency balance responses, such that the high frequency balance responses of the cerebellum are not necessary during the SR visual condition. The somatosensory system can use passive mechanical properties or use information from the deformation of soft tissue. Further, the vestibular system can detect head motion, orientation, and rotation in relation

to gravity. These mechanisms of the somatosensory and vestibular systems can induce postural sway at frequencies below the medium frequency band [46].

On the foam surface, the AP COP and AP COM identified an increase between EO and EC, AMP, and SR visual conditions. This result demonstrated that when two of three sensory systems are altered, the sensory reweighting processes increased medium frequency band composition, which can be explained by the processes of the cerebellum. The cerebellum is not a sensory system, but rather integrates sensory information from the visual, vestibular, and somatosensory to error correct and provide feed-forward control, necessary processes to maintain upright stance when there is sensory conflict. For example, on the firm surface, there was a decrease in medium frequency band composition for SR, likely due to the upweighting of somatosensory information, but when standing on foam, there is a disproportionate increase in medium frequency band composition for the AP COP and AP COM. The combination of increased ankle torque variability needed to stand on the foam surface and removed motion cues in the visual environment during the SR visual condition creates an increased need for error correction via the cerebellum and detection of body motion via the vestibular system. This same logic can be applied to EC and AMP vision on the foam surface.

Overall, the processes of the cerebellum can be related to medium frequency band composition; however, the cerebellum cannot influence postural control without the influence of afferent sensory information. Visual, vestibular and somatosensory inputs influence the extent to which the processes of the cerebellum contribute to medium frequency band composition. Right soleus muscle activity showed a statistical difference between EO and EC visual conditions, but no other difference was identified. The results of this thesis show that muscle activity increased during EC and during surface change in the medium frequency band, which is congruent with

literature that has demonstrated increased muscle activity with a change in support surface and removal of visual information [17,91].

Taken together, the results within the medium frequency band demonstrated that the FSCF can provide an explanation for the cerebellum's contribution to upright stance but does not account for the direct influence of visual, vestibular, and somatosensory information on medium frequency band composition. This suggests that the processes of the cerebellum are relevant to upright stance; however, the conclusions made by the FSCF disregard the influence of afferent sensory information has on the processes of the cerebellum during upright stance. This makes the interpretations of the FSCF too simplistic to describe the mechanisms influencing the medium frequency band.

4.2.4 High Frequency Band

The high frequency band (1-5Hz) has been related to the somatosensory contribution to upright stance [48,92]. The somatosensory system contributes reflexive postural adjustments, and transmits balance relevant information to supraspinal structures such as the brainstem, cerebellum, thalamus and somatosensory cortex [1,45]. Somatosensory input from the feet and lower limbs informs the CNS of body orientation and support surface conditions, enabling precise modulation of postural muscle activity [4]. Previous work supports somatosensory contributions to upright stance in the high frequency band, showing that reducing leg afferent input through ischemia increased postural instability above 1Hz [92]. Further, previous work also showed that standing on an unstable surface is mediated by segmental stretch reflex activity [48]. This evidence is the basis of the high frequency band, and when using the FSCF to interpret somatosensory contributions to upright stance, a 1-5Hz frequency range is used.

The high frequency band demonstrated the same results as the medium frequency band for all dependent measures for the AP COP, AP COM, and right soleus. The only exception was for AP COP, where there was no statistical difference between AMP and SR visual conditions on the firm surface. The FSCF would predict that when a sensory system is made unreliable, there should be a decrease in relative frequency contribution; however, this result between AMP and SR shows the opposite outcome. For example, the logic for the ultra-low frequency band associated with the visual contributions to upright stance used evidence showing that removed vision shifted frequency power outside of the ultra-low frequency band [62,92]. The results of this thesis indicated that when participants stood on foam (made somatosensory information unreliable), there was an increase in all the dependent measures, the opposite of what the FSCF would have predicted.

In the literature, high frequency balance control has been associated with spinal reflexes and other spinal cord related mechanisms directly related to the somatosensory system [48]. However, evidence for the FSCF does not consider the passive control of the musculotendinous structures. Passive mechanical properties and tonic muscle activation, part of the somatosensory system, contribute to postural sway in frequency bands below the high frequency band [93].

Furthermore, low- and high frequency postural control mechanisms parallel the behaviour of fast and slow-adapting mechanoreceptors in the plantar surface [47,94]. In the literature, mechanisms that support high frequency balance control include spinal reflexes, which can use information from the vestibular systems via the vestibular spinal reflex as well as proprioceptive information from the stretch reflex [95,96]. The results in the high frequency band suggest that there is overlap between the control mechanisms of the medium and high frequency bands, evidenced by similar results across the dependent variables for the medium and high

frequency bands. For example, EC, AMP, and SR visual conditions increased on the foam surface compared to EO on foam. Further, EC, AMP, and SR firm surface conditions, compared to the matched visual condition on the foam surface, increased for both the AP COP and AP COM in the medium- and high frequency bands. This suggests that pathways postulated to only exist above 1Hz may not be defined as contributions of the somatosensory system. Medium- and high frequency balance control mechanisms may overlap, and similar control strategies may be used above 0.5Hz. The sharing of these faster mechanics may be due to the dynamic reweighting of afferent sensory information which modulates muscular activity across a greater range of frequencies.

The evidence of this thesis suggests that the FSCF does not accurately describe the somatosensory system's contribution to upright stance. Overall, the FSCF does not account for the low frequency applications of the somatosensory system, only accounting for the contributions above 1Hz. Thus, making the interpretations of frequency data related to the somatosensory system inaccurate, and neglecting the influence other sensory systems may have during high frequency upright stance control.

4.3 Limitations & Future Work

This work is not without limitations. First, a healthy young adult population was recruited and applied in analysis; thus, the interpretations and effects of the sensory manipulations done in this study may not be generalizable across populations. Future work should examine the integrity of the FCSF in older adult populations to assess its robustness with aging. In terms of data collection, this study used a foam pad to simulate nullification of ankle proprioception. Using a SR platform may induce greater unreliability of somatosensory information related to balance and maintain a consistent level of sensory alteration across participants. Finally, this work did not

include a mediolateral (ML) analysis of the COP or COM, nor the analysis of ML-related muscles or other dorsi- and plantar flexor muscles associated with the maintenance of upright stance. These variables may provide further evidence and a deeper understanding of the behavioural outcomes when sensory information is manipulated, which may provide insight into frequency related strategies of upright stance.

Chapter 5: Conclusions

The purpose of this thesis was to critically examine and challenge the FSCF to improve the characterization of how sensory information shapes and regulates balance control using a novel Virtual Reality-Sensory Interaction Balance Test. In this thesis, it was shown that sensory information extended beyond the hypothesized frequency bands defined by the FSCF. Future work examining the frequency specific sensory contributions to balance should be cautious in associating sensory inputs with FSCF-postulated frequency bands across kinetic, kinematic, and muscle activity variables. It was found that the visual contributions to balance extend beyond the ultra-low frequency band and that somatosensory contributions extended below the high frequency band. Furthermore, this dataset informs an alternative framework for characterizing frequency-based postural control strategies, which may provide a more robust understanding of the frequency-specific mechanisms associated with the maintenance of upright stance. Overall, this work suggests that interpreting sensory contributions to upright stance based on only the FSCF may be an oversimplification of understanding the sensory contributions to balance.

5.1 A Proposed Framework: Low & High Frequency Control

Based on the results of this study, the FSCF was not robust to describe the complexity of frequency-specific sensory contributions to the maintenance of upright stance. This thesis provided evidence that the sensory contributions to upright stance cannot be solely described through and associated with specific frequency outputs. Informed by these findings, an alternative framework for sensory contributions to upright stance is proposed, involving a two-domain model which separates frequency outputs into low (0-0.5Hz) and high frequency (0.5-5Hz) control strategies. Refer to Appendix C for figures showing the low and high frequency control framework.

In this thesis, it was evidenced that sensory information influences upright stance across the range of frequencies (0-5Hz) and that sensory information was used to optimally maintain upright stance with a prioritization for visual and low frequency control. The proposed low frequency domain extends from 0-0.5Hz, which makes up roughly 90% of frequency information according to the results of this thesis and previous work [97]. The high frequency domain extends from 0.5-5Hz as evidence in this thesis suggested that similar mechanisms of upright stance were being used for high frequency balance control (*section 4.2.3 & 4.2.4*).

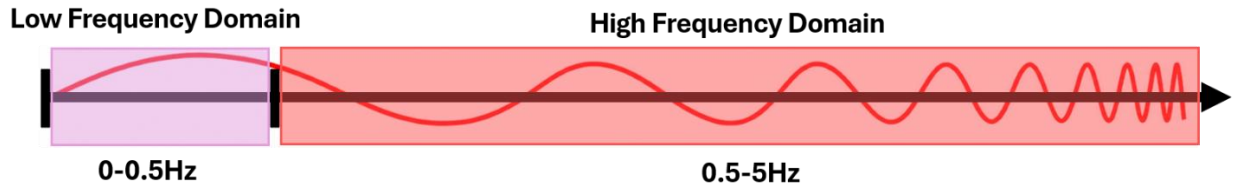

Figure 19: *The Low and High Frequency Control Framework*

5.1.2 Low Frequency Domain

The proposed low frequency domain extends from 0-0.5Hz. The low frequency domain represents a slow and low frequency balance control system including external spatial reference cues about the body's orientation and motion relative to the surrounding environment, a function of the visual system. Further, it includes functions of the vestibular system, which estimate head and upper-body motion relative to gravity, as well as passive and slow-adapting mechanoreceptors in the plantar surface, a function of the somatosensory system.

This low frequency domain is informed by the outcomes of this thesis. For example, on the firm surface, low frequency control was maintained across visual conditions, suggesting that vestibular and somatosensory inputs were reweighted when visual information was altered. In

this case, the process of sensory reweighting can be associated with increased information for cutaneous mechanoreceptors and passive musculotendinous control, and detection of linear motion via the vestibular system's otolith organs. In other work examining slow and low frequency control mechanisms, it was found that humans use integrated force afferents from the feet and legs in a slow, positive feedback mechanism during standing to remain upright [98]. Integrated force afferents include signals sourced from mechanoreceptors sensing pressure under the feet, Golgi tendon organs in the ankle plantarflexors, or intrinsic muscle spindles in the foot [98]. These mechanisms operate across a range of frequencies [99], which implies a low-pass filter in the central processing mechanism [98]. Low frequency control is emphasized as the COM is constrained by the COP and the inertial properties of the inverted pendulum [78] and reflects both the mechanical and feedback properties of the postural control system [2,98,100]. Low frequency balance control encompasses all sensory information, including somatosensory information, which was omitted from low frequency control in the FSCF.

5.1.3 High Frequency Domain

The proposed high frequency domain extends from 0.5-5Hz. The high frequency domain represents a rapid balance control system including spinal reflexes, short and long latency responses of the stretch reflex, and contributions of the cerebellum influenced by visual, vestibular, and somatosensory inputs [34,58]. Together, these mechanisms aid in the maintenance of upright stance and make postural control adaptive across sensory and mechanical manipulation. This high frequency control may be used in challenging situations, such as when sensory information is altered, removed or made unreliable.

In this thesis, the AP COP and AP COM increased on a foam surface with manipulated vision (EC, AMP, and SR) in the medium and high frequency band. Furthermore, there was an

increase in total band power during altered visual conditions on the foam surface, which provides evidence for a shift in postural strategy associated with the maintenance of upright stance during challenging sensory conditions. Increases in compositional and absolute frequency information cannot be postulated to specific sensory systems; instead, a combination of neural mechanisms can be used to describe these adaptations from low to high frequency control. For example, during AMP visual conditions, vision may influence postural control above 0.5Hz via the selection and scaling of muscle activation [101]. The results of this data show that future interpretations of frequency specific balance control should refer to specific neural pathways associated with sensory manipulation, which can be interpreted as low and high frequency domains of upright stance control.

Overall, the low and high frequency control framework provides a more comprehensive understanding of how frequency related outputs relate to postural control mechanisms. Further, the low and high frequency control framework includes how the visual, vestibular, and somatosensory systems can influence upright stance across multiple frequency domains. Interpreting frequency data associated with low and high frequency domains may provide a more accurate understanding of the neural mechanisms associated with the control of upright stance.

References

1. Peterka, R. J. (2002). Sensorimotor Integration in Human Postural Control. *Journal of Neurophysiology*, *88*(3), 1097–1118. https://doi.org/10.1152/jn.2002.88.3.1097
2. Assländer, L., & Peterka, R. J. (2014). Sensory reweighting dynamics in human postural control. *Journal of Neurophysiology*, *111*(9), 1852–1864. https://doi.org/10.1152/jn.00669.2013
3. Kuo, A. D. (1995). An optimal control model for analyzing human postural balance. *IEEE Transactions on Biomedical Engineering*, *42*(1), 87–101. https://doi.org/10.1109/10.362914
4. Winter, D. (1995). Human balance and posture control during standing and walking. *Gait & Posture*, *3*(4), 193–214. https://doi.org/10.1016/0966-6362(96)82849-9
5. Gage, W. H., Winter, D. A., Frank, J. S., & Adkin, A. L. (2004). Kinematic and kinetic validity of the inverted pendulum model in quiet standing. *Gait & Posture*, *19*(2), 124–132. https://doi.org/10.1016/S0966-6362(03)00037-7
6. Horak, F. B. (2006). Postural orientation and equilibrium: What do we need to know about neural control of balance to prevent falls? *Age and Ageing*, *35*(suppl_2), ii7–ii11. https://doi.org/10.1093/ageing/afl077
7. Laessoe, U., & Voigt, M. (2008). Anticipatory postural control strategies related to predictive perturbations. *Gait & Posture*, *28*(1), 62–68. https://doi.org/10.1016/j.gaitpost.2007.10.001
8. Hsu, W.-L., Scholz, J. P., Schöner, G., Jeka, J. J., & Kiemel, T. (2007). Control and Estimation of Posture During Quiet Stance Depends on Multijoint Coordination. *J Neurophysiol*, *97*.
9. Grove, C. R., Whitney, S. L., Hetzel, S. J., Heiderscheit, B. C., & Pyle, G. M. (2021). Validation of a next-generation sensory organization test in adults with and without

vestibular dysfunction. *Journal of Vestibular Research*, *31*(1), 33–45. https://doi.org/10.3233/VES-200040

10. Nashner, L., Black, F., & Wall, C. (1982). Adaptation to altered support and visual conditions during stance: Patients with vestibular deficits. *The Journal of Neuroscience*, *2*(5), 536–544. https://doi.org/10.1523/JNEUROSCI.02-05-00536.1982
11. Doumas, M., Valkanidis, T. Ch., & Hatzitaki, V. (2019). Putting proprioception for balance to the test: Contrasting and combining sway referencing and tendon vibration. *Gait & Posture*, *67*, 201–206. https://doi.org/10.1016/j.gaitpost.2018.10.012
12. Cohen, H., Heaton, L. G., Congdon, S. L., & Jenkins, H. A. (1996). Changes in Sensory Organization Test Scores with Age. *Age and Ageing*, *25*(1), 39–44. https://doi.org/10.1093/ageing/25.1.39
13. Shumway-Cook, A., & Horak, F. B. (1986). Assessing the Influence of Sensory Interaction on Balance: Suggestion from the Field. *Physical Therapy*, *66*(10), 1548–1550. https://doi.org/10.1093/ptj/66.10.1548
14. Horn, L. B., Rice, T., Stoskus, J. L., Lambert, K. H., Dannenbaum, E., & Scherer, M. R. (2015). Measurement Characteristics and Clinical Utility of the Clinical Test of Sensory Interaction on Balance (CTSIB) and Modified CTSIB in Individuals With Vestibular Dysfunction. *Archives of Physical Medicine and Rehabilitation*, *96*(9), 1747–1748. https://doi.org/10.1016/j.apmr.2015.04.003
15. Patel, M., Fransson, P. A., Lush, D., & Gomez, S. (2008). The effect of foam surface properties on postural stability assessment while standing. *Gait & Posture*, *28*(4), 649–656. https://doi.org/10.1016/j.gaitpost.2008.04.018

16. Mohapatra, S., Kukkar, K. K., & Aruin, A. S. (2014). Support surface related changes in feedforward and feedback control of standing posture. *Journal of Electromyography and Kinesiology*, *24*(1), 144–152. https://doi.org/10.1016/j.jelekin.2013.10.015
17. Fransson, P. A., Gomez, S., Patel, M., & Johansson, L. (2007). Changes in multi-segmented body movements and EMG activity while standing on firm and foam support surfaces. *European Journal of Applied Physiology*, *101*(1), 81–89. https://doi.org/10.1007/s00421-007-0476-x
18. Chiang, J.-H., & Wu, G. (1997). The influence of foam surfaces on biomechanical variables contributing to postural control. *Gait & Posture*, *5*(3), 239–245. https://doi.org/10.1016/S0966-6362(96)01091-0
19. Assländer, L., & Streuber, S. (2020). Virtual reality as a tool for balance research: Eyes open body sway is reproduced in photo-realistic, but not in abstract virtual scenes. *PLOS ONE*, *15*(10), e0241479. https://doi.org/10.1371/journal.pone.0241479
20. Hwang, S., Agada, P., Kiemel, T., & Jeka, J. J. (2014). Dynamic Reweighting of Three Modalities for Sensor Fusion. *PLoS ONE*, *9*(1), e88132. https://doi.org/10.1371/journal.pone.0088132
21. Nishiike, S., Okazaki, S., Watanabe, H., Akizuki, H., Imai, T., Uno, A., Kitahara, T., Horii, A., Takeda, N., & Inohara, H. (2013). The effect of visual-vestibulosomatosensory conflict induced by virtual reality on postural stability in humans. *The Journal of Medical Investigation*, *60*(3.4), 236–239. https://doi.org/10.2152/jmi.60.236
22. Redfern, M. S., Yardley, L., & Bronstein, A. M. (2001). Visual influences on balance. *Journal of Anxiety Disorders*, *15*(1–2), 81–94. https://doi.org/10.1016/S0887-6185(00)00043-8

23. Mather, G., Pavan, A., Bellacosa Marotti, R., Campana, G., & Casco, C. (2013). Interactions between motion and form processing in the human visual system. *Frontiers in Computational Neuroscience*, *7*. https://doi.org/10.3389/fncom.2013.00065
24. Niehorster, D. C. (2021). Optic Flow: A History. *I-Perception*, *12*(6), 20416695211055766. https://doi.org/10.1177/20416695211055766
25. Lappe, M., Bremmer, F., & Van Den Berg, A. V. (1999). Perception of self-motion from visual flow. *Trends in Cognitive Sciences*, *3*(9), 329–336. https://doi.org/10.1016/S1364-6613(99)01364-9
26. Lavalle, L. K., & Cleworth, T. W. (2023). The effect of modified optic flow gain on quiet stance. *Neuroscience Letters*, *797*, 137068. https://doi.org/10.1016/j.neulet.2023.137068
27. Pourhashemi, N., & Cleworth, T. W. (2025). Exploring the role of reduced optic flow in dynamic balance. *Gait & Posture*, *118*, 148–153. https://doi.org/10.1016/j.gaitpost.2025.02.007
28. Horak, F. B., Nashner, L. M., & Diener, H. C. (1990). Postural strategies associated with somatosensory and vestibular loss. *Experimental Brain Research*, *82*(1). https://doi.org/10.1007/BF00230848
29. Assländer, L., Albrecht, M., Diehl, M., Missen, K. J., Carpenter, M. G., & Streuber, S. (2023). Estimation of the visual contribution to standing balance using virtual reality. *Scientific Reports*, *13*(1), 2594. https://doi.org/10.1038/s41598-023-29713-7
30. Dichgans, J., Mauritz, K. H., Allum, J. H., & Brandt, T. (1976). Postural sway in normals and atactic patients: Analysis of the stabilising and destabilizing effects of vision. *Agressologie: Revue Internationale De Physio-Biologie Et De Pharmacologie Appliquees Aux Effets De L'agression*, *17*(C Spec No), 15–24.

31. Lestienne, F., Soechting, J., & Berthoz, A. (1977). Postural readjustments induced by linear motion of visual scenes. *Experimental Brain Research*, *28–28*(3–4). https://doi.org/10.1007/BF00235717

32. Lin, I.-S., Lai, D.-M., Ding, J.-J., Chien, A., Cheng, C.-H., Wang, S.-F., Wang, J.-L., Kuo, C.-L., & Hsu, W.-L. (2019). Reweighting of the sensory inputs for postural control in patients with cervical spondylotic myelopathy after surgery. *Journal of NeuroEngineering and Rehabilitation*, *16*, 96. https://doi.org/10.1186/s12984-019-0564-2

33. Friedrich, M., Grein, H.-J., Wicher, C., Schuetze, J., Mueller, A., Lauenroth, A., Hottenrott, K., & Schwesig, R. (2008). Influence of pathologic and simulated visual dysfunctions on the postural system. *Experimental Brain Research*, *186*(2), 305–314. https://doi.org/10.1007/s00221-007-1233-4

34. Takakusaki, K. (2017). Functional Neuroanatomy for Posture and Gait Control. *Journal of Movement Disorders*, *10*(1), 1–17. https://doi.org/10.14802/jmd.16062

35. McCall, A. A., Miller, D. M., & Yates, B. J. (2017). Descending Influences on Vestibulospinal and Vestibulosympathetic Reflexes. *Frontiers in Neurology*, *8*, 112. https://doi.org/10.3389/fneur.2017.00112

36. Maurer, C., Mergner, T., Bolha, B., & Hlavacka, F. (2000). Vestibular, visual, and somatosensory contributions to human control of upright stance. *Neuroscience Letters*, *281*(2–3), 99–102. https://doi.org/10.1016/S0304-3940(00)00814-4

37. Drake, R., Vogl, A. W., & Mitchell, A. W. M. (2009). *Gray's Anatomy for Students E-Book*. Elsevier Health Sciences.

38. Nashner, L. M. (1971). A Model Describing Vestibular Detection of Body Sway Motion. *Acta Oto-Laryngologica*, *72*(1–6), 429–436. https://doi.org/10.3109/00016487109122504

39. Meiry, J. L. (n.d.). *THE VESTIBULAR SYSTEM AND HUMAN DYNAMIC SPACE ORIENTATION*.

40. Cathers, I., Day, B. L., & Fitzpatrick, R. C. (2005). Otolith and canal reflexes in human standing. *The Journal of Physiology*, *563*(Pt 1), 229–234. https://doi.org/10.1113/jphysiol.2004.079525

41. Horak, F. B., Shupert, C. L., Dietz, V., & Horstmann, G. (1994). Vestibular and somatosensory contributions to responses to head and body displacements in stance. *Experimental Brain Research*, *100*(1). https://doi.org/10.1007/BF00227282

42. Fitzpatrick, R. C., & Day, B. L. (2004). Probing the human vestibular system with galvanic stimulation. *Journal of Applied Physiology*, *96*(6), 2301–2316. https://doi.org/10.1152/japplphysiol.00008.2004

43. Kapteyn, T. S., & Wit, G. de. (1972). Posturography as an Auxiliary in Vestibular Investigation. *Acta Oto-Laryngologica*, *73*(2–6), 104–111. https://doi.org/10.3109/00016487209138918

44. Massion, J. (1994). Postural control system. *Current Opinion in Neurobiology*, *4*(6), 877–887. https://doi.org/10.1016/0959-4388(94)90137-6

45. Proske, U., & Gandevia, S. C. (2012). The proprioceptive senses: Their roles in signaling body shape, body position and movement, and muscle force. *Physiological Reviews*, *92*(4), 1651–1697. https://doi.org/10.1152/physrev.00048.2011

46. Winter, D. A., Patla, A. E., Prince, F., Ishac, M., & Gielo-Perczak, K. (1998). Stiffness Control of Balance in Quiet Standing. *Journal of Neurophysiology*, *80*(3), 1211–1221. https://doi.org/10.1152/jn.1998.80.3.1211

47. Dougla, S. (n.d.). *THE ROLE OF PLANTAR CUTANEOUS MECHANORECEPTORSIN THE CONTROL OF COMPENSATORY STEPPING IN THE YOUNG AND OLDER ADULT.*

48. Dietz, V., Mauritz, K.-H., & Dichgans, J. (1980). Body oscillations in balancing due to segmental stretch reflex activity. *Experimental Brain Research*, *40*(1). https://doi.org/10.1007/BF00236666

49. Goodworth, A. D., & Peterka, R. J. (2012). Sensorimotor integration for multisegmental frontal plane balance control in humans. *Journal of Neurophysiology*, *107*(1), 12–28. https://doi.org/10.1152/jn.00670.2010

50. Missen, K. J., Carpenter, M. G., & Assländer, L. (2024). Velocity dependence of sensory reweighting in human balance control. *Journal of Neurophysiology*, *132*(2), 454–460. https://doi.org/10.1152/jn.00075.2024

51. Oie, K. S., Kiemel, T., & Jeka, J. J. (2002). Multisensory fusion: Simultaneous re-weighting of vision and touch for the control of human posture. *Cognitive Brain Research*, *14*(1), 164–176. https://doi.org/10.1016/S0926-6410(02)00071-X

52. Ting, L. H., & Macpherson, J. M. (2005). A Limited Set of Muscle Synergies for Force Control During a Postural Task. *Journal of Neurophysiology*, *93*(1), 609–613. https://doi.org/10.1152/jn.00681.2004

53. Fitzpatrick, R. C., Taylor, J. L., & McCloskey, D. I. (1992). Ankle stiffness of standing humans in response to imperceptible perturbation: Reflex and task-dependent components. *The Journal of Physiology*, *454*(1), 533–547. https://doi.org/10.1113/jphysiol.1992.sp019278

54. Diener, H. C., Dichgans, J., Bacher, M., & Gompf, B. (1984). Quantification of postural sway in normals and patients with cerebellar diseases. *Electroencephalography and Clinical Neurophysiology*, *57*(2), 134–142. https://doi.org/10.1016/0013-4694(84)90172-X

55. Cullen, K. E. (2019). Vestibular processing during natural self-motion: Implications for perception and action. *Nature Reviews Neuroscience*, *20*(6), 346–363. https://doi.org/10.1038/s41583-019-0153-1

56. Schepens, B., & Drew, T. (2004). Independent and Convergent Signals From the Pontomedullary Reticular Formation Contribute to the Control of Posture and Movement During Reaching in the Cat. *Journal of Neurophysiology*, *92*(4), 2217–2238. https://doi.org/10.1152/jn.01189.2003

57. Asan, A. S., McIntosh, J. R., & Carmel, J. B. (2022). Targeting Sensory and Motor Integration for Recovery of Movement After CNS Injury. *Frontiers in Neuroscience*, *15*, 791824. https://doi.org/10.3389/fnins.2021.791824

58. Morton, S. M., & Bastian, A. J. (2004). Cerebellar Control of Balance and Locomotion. *The Neuroscientist*, *10*(3), 247–259. https://doi.org/10.1177/1073858404263517

59. *1984 H C Diener—Quantification of postural sway in normals and pat [retrieved_2026-03-24]*. (n.d.).

60. Maki, B. E., & McIlroy, W. E. (2007). Cognitive demands and cortical control of human balance-recovery reactions. *Journal of Neural Transmission*, *114*(10), 1279–1296. https://doi.org/10.1007/s00702-007-0764-y

61. Limanowski, J., & Friston, K. (2020). Attentional Modulation of Vision Versus Proprioception During Action. *Cerebral Cortex*, *30*(3), 1637–1648. https://doi.org/10.1093/cercor/bhz192

62. Mauritz, K.-H., & Dietz, V. (1980). Characteristics of postural instability induced by ischemic blocking of leg afferents. *Experimental Brain Research*, *38*(1). https://doi.org/10.1007/BF00237939

63. Nashner, L. M., Shupert, C. L., Horak, F. B., & Black, F. O. (1989). Chapter 33 Organization of posture controls: An analysis of sensory and mechanical constraints. In J. H. J. Allum & M. Hulliger (Eds.), *Progress in Brain Research* (Vol. 80, pp. 411–418). Elsevier. https://doi.org/10.1016/S0079-6123(08)62237-2

64. Fujimoto, C., Kamogashira, T., Kinoshita, M., Egami, N., Sugasawa, K., Demura, S., Yamasoba, T., & Iwasaki, S. (2014). Power spectral analysis of postural sway during foam posturography in patients with peripheral vestibular dysfunction. *Otology & Neurotology: Official Publication of the American Otological Society, American Neurotology Society [and] European Academy of Otology and Neurotology*, *35*(10), e317-323. https://doi.org/10.1097/MAO.0000000000000554

65. Allum, J. H. J., Zamani, F., Adkin, A. L., & Ernst, A. (2002). Differences between trunk sway characteristics on a foam support surface and on the Equitest® ankle-sway-referenced support surface. *Gait & Posture*, *16*(3), 264–270. https://doi.org/10.1016/S0966-6362(02)00011-5

66. Liang, Z. (n.d.). *Neck musculature fatigue affects specific frequency bands of postural dynamics during quiet standing*.

67. Karmali, F., Goodworth, A. D., Valko, Y., Leeder, T., Peterka, R. J., & Merfeld, D. M. (2021). The role of vestibular cues in postural sway. *Journal of Neurophysiology*, *125*(2), 672–686. https://doi.org/10.1152/jn.00168.2020

68. Schut, I. M., Engelhart, D., Pasma, J. H., Aarts, R. G. K. M., & Schouten, A. C. (2017). Compliant support surfaces affect sensory reweighting during balance control. *Gait & Posture*, *53*, 241–247. https://doi.org/10.1016/j.gaitpost.2017.02.004

69. Creath, R., Kiemel, T., Horak, F., Peterka, R., & Jeka, J. (2005). A unified view of quiet and perturbed stance: Simultaneous co-existing excitable modes. *Neuroscience Letters*, *377*(2), 75–80. https://doi.org/10.1016/j.neulet.2004.11.071

70. Carver, S., Kiemel, T., & Jeka, J. J. (2006). Modeling the Dynamics of Sensory Reweighting. *Biological Cybernetics*, *95*(2), 123–134. https://doi.org/10.1007/s00422-006-0069-5

71. Assländer, L., Hettich, G., & Mergner, T. (2015). Visual contribution to human standing balance during support surface tilts. *Human Movement Science*, *41*, 147–164. https://doi.org/10.1016/j.humov.2015.02.010

72. Horak, F. B., & Nashner, L. M. (n.d.). *Central programming of postural movements: Adaptation to altered support-surface configurations*.

73. Meyer, J. (1999). *Standards for Reporting EMG Data*.

74. Esposito, D., Centracchio, J., Bifulco, P., & Andreozzi, E. (2023). A smart approach to EMG envelope extraction and powerful denoising for human–machine interfaces. *Scientific Reports*, *13*(1), 7768. https://doi.org/10.1038/s41598-023-33319-4

75. *Bandpower—Band power—MATLAB*. (n.d.). Retrieved May 14, 2026, from https://www.mathworks.com/help/releases/R2024b/signal/ref/bandpower.html

76. Fujimoto, C., Egami, N., Demura, S., Yamasoba, T., & Iwasaki, S. (2015). The effect of aging on the center-of-pressure power spectrum in foam posturography. *Neuroscience Letters*, *585*, 92–97. https://doi.org/10.1016/j.neulet.2014.11.033

77. Peterka, RobertJ., & Benolken, MarthaS. (1995). Role of somatosensory and vestibular cues in attenuating visually induced human postural sway. *Experimental Brain Research*, *105*(1). https://doi.org/10.1007/BF00242186

78. Winter, D. A., Prince, F., Frank, J. S., Powell, C., & Zabjek, K. F. (1996). Unified theory regarding A/P and M/L balance in quiet stance. *Journal of Neurophysiology*, *75*(6), 2334–2343. https://doi.org/10.1152/jn.1996.75.6.2334

79. Dewan, B. M., James, C. R., Kumar, N. A., Burgess, N., Zupancic, S., & Sawyer, S. F. (2023). Adaptation in motor strategies for postural control associated with sensory reweighting. *Human Movement Science*, *89*, 103098. https://doi.org/10.1016/j.humov.2023.103098

80. Mochizuki, G., Semmler, J. G., Ivanova, T. D., & Garland, S. J. (2006). Low frequency common modulation of soleus motor unit discharge is enhanced during postural control in humans. *Experimental Brain Research*, *175*(4), 584–595. https://doi.org/10.1007/s00221-006-0575-7

81. Moritani, T., Oddsson, L., & Thorstensson, A. (1991). Activation patterns of the soleus and gastrocnemius muscles during different motor tasks. *Journal of Electromyography and Kinesiology*, *1*(2), 81–88. https://doi.org/10.1016/1050-6411(91)90001-L

82. Kuo, A. D., Speers, R. A., Peterka, R. J., & Horak, F. B. (1998). Effect of altered sensory conditions on multivariate descriptors of human postural sway. *Experimental Brain Research*, *122*(2), 185–195. https://doi.org/10.1007/s002210050506

83. Amblard, B., Cr□mieux, J., Marchand, A. R., & Carblanc, A. (1985). Lateral orientation and stabilization of human stance: Static versus dynamic visual cues. *Experimental Brain Research*, *61*(1). https://doi.org/10.1007/BF00235617

84. Winter, D. A., Patla, A. E., Rietdyk, S., & Ishac, M. G. (2001). Ankle Muscle Stiffness in the Control of Balance During Quiet Standing. *Journal of Neurophysiology*, *85*(6), 2630–2633. https://doi.org/10.1152/jn.2001.85.6.2630

85. Loram, I. D., Maganaris, C. N., & Lakie, M. (2005). Human postural sway results from frequent, ballistic bias impulses by soleus and gastrocnemius. *The Journal of Physiology*, *564*(1), 295–311. https://doi.org/10.1113/jphysiol.2004.076307

86. Lavalle, L. K., Lipson, A., Weinberg, S. E., & Cleworth, T. W. (2025). Examining the contributions of radial and lamellar optic flow gain to quiet stance. *Scientific Reports*, *15*(1), 19638. https://doi.org/10.1038/s41598-025-03648-7

87. Dokka, K., DeAngelis, G. C., & Angelaki, D. E. (2015). Multisensory Integration of Visual and Vestibular Signals Improves Heading Discrimination in the Presence of a Moving Object. *The Journal of Neuroscience*, *35*(40), 13599–13607. https://doi.org/10.1523/JNEUROSCI.2267-15.2015

88. Paige, G. D., Telford, L., Seidman, S. H., & Barnes, G. R. (1998). Human Vestibuloocular Reflex and Its Interactions With Vision and Fixation Distance During Linear and Angular Head Movement. *Journal of Neurophysiology*, *80*(5), 2391–2404. https://doi.org/10.1152/jn.1998.80.5.2391

89. Ioffe, M. E., Chernikova, L. A., & Ustinova, K. I. (2007). Role of cerebellum in learning postural tasks. *The Cerebellum*, *6*(1), 87. https://doi.org/10.1080/14734220701216440

90. Singh, N. B., Taylor, W. R., Madigan, M. L., & Nussbaum, M. A. (2012). The spectral content of postural sway during quiet stance: Influences of age, vision and somatosensory inputs. *Journal of Electromyography and Kinesiology*, *22*(1), 131–136. https://doi.org/10.1016/j.jelekin.2011.10.007

91. Patel, M., Gomez, S., Lush, D., & Fransson, P. A. (2009). Adaptation and vision change the relationship between muscle activity of the lower limbs and body movement during human

balance perturbations. *Clinical Neurophysiology*, *120*(3), 601–609. https://doi.org/10.1016/j.clinph.2008.11.026

92. Diener, H. C., Dichgans, J., Guschlbauer, B., & Mau, H. (1984). The significance of proprioception on postural stabilization as assessed by ischemia. *Brain Research*, *296*(1), 103–109. https://doi.org/10.1016/0006-8993(84)90515-8
93. Winter, D. A., Patla, A. E., Prince, F., Ishac, M., & Gielo-Perczak, K. (1998). Stiffness Control of Balance in Quiet Standing. *Journal of Neurophysiology*, *80*(3), 1211–1221. https://doi.org/10.1152/jn.1998.80.3.1211
94. Kavounoudias, A., Roll, R., & Roll, J.-P. (1998). The plantar sole is a 'dynamometric map' for human balance control: *NeuroReport*, *9*(14), 3247–3252. https://doi.org/10.1097/00001756-199810050-00021
95. Horslen, B. C., Zaback, M., Inglis, J. T., Blouin, J., & Carpenter, M. G. (2018). Increased human stretch reflex dynamic sensitivity with height-induced postural threat. *The Journal of Physiology*, *596*(21), 5251–5265. https://doi.org/10.1113/JP276459
96. Forbes, P. A., Siegmund, G. P., Schouten, A. C., & Blouin, J.-S. (2015). Task, muscle and frequency dependent vestibular control of posture. *Frontiers in Integrative Neuroscience*, *8*. https://doi.org/10.3389/fnint.2014.00094
97. Soames, R. W., & Atha, J. (1982). The spectral characteristics of postural sway behaviour. *European Journal of Applied Physiology and Occupational Physiology*, *49*(2), 169–177. https://doi.org/10.1007/BF02334065
98. Missen, K. J., Carpenter, M. G., & Assländer, L. (2025). Slow dynamics of human balance control. *Scientific Reports*, *15*(1), 27593. https://doi.org/10.1038/s41598-025-09392-2

99. Magnusson, M., Enbom, H., Johansson, R., & Wiklund, J. (1990). Significance of pressor input from the human feet in lateral postural control: The Effect of Hypothermia on Galvanically Induced Body-sway. *Acta Oto-Laryngologica*, *110*(5–6), 321–327. https://doi.org/10.3109/00016489009107450

100. Missen, K. J., Assländer, L., Babichuk, A., Chua, R., Inglis, J. T., & Carpenter, M. G. (2023). The role of torque feedback in standing balance. *Journal of Neurophysiology*, *130*(3), 585–595. https://doi.org/10.1152/jn.00046.2023

101. Buchanan, J. J., & Horak, F. B. (1999). Emergence of Postural Patterns as a Function of Vision and Translation Frequency. *Journal of Neurophysiology*, *81*(5), 2325–2339. https://doi.org/10.1152/jn.1999.81.5.2325

Appendix A: AP COP FSCF Predictions vs Actual Results per condition

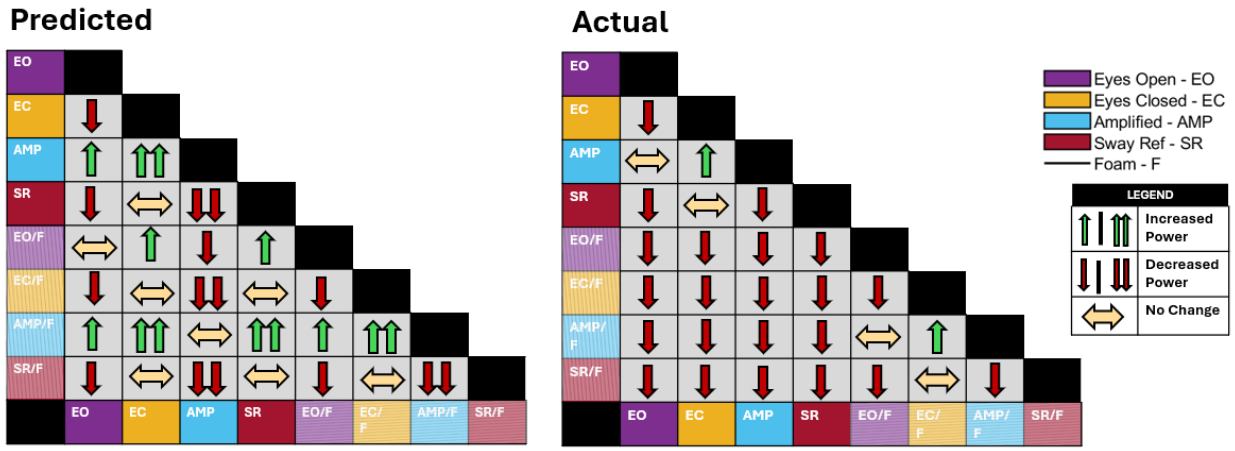

Figure 20: *This figure displays the FSCF-predicted responses (left) and the actual results (right) for the ultra-low frequency band (0-0.1Hz) for AP COP. To interpret this figure, the condition on the y-axis is compared to the subsequent condition on the x-axis. The legends indicate both the condition and the direction of change. Hatched boxes indicate foam surface conditions. A single arrow indicates a predicted increase or decrease, whereas a double arrow indicates a stronger predicted change supported by changes in more than one variable.*

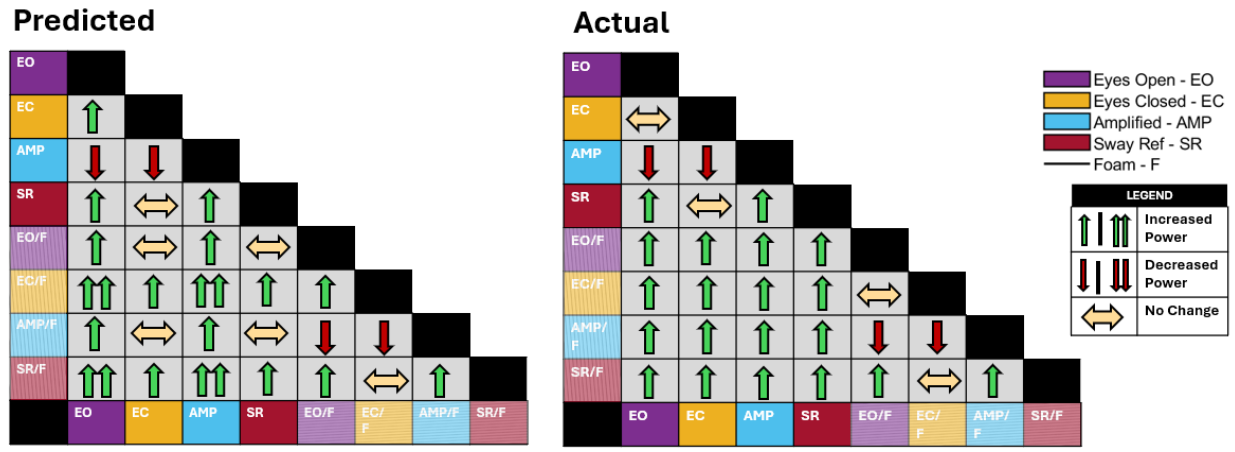

Figure 21: *This figure displays the FSCF-predicted responses (left) and the actual results (right) for the low frequency band (0.1-0.5Hz) for AP COP. To interpret this figure, the condition on the y-axis is compared to the subsequent condition on the x-axis. The legends indicate both the condition and the direction of change. Hatched boxes indicate foam surface conditions. A single arrow indicates a predicted increase or decrease, whereas a double arrow indicates a stronger predicted change supported by changes in more than one variable.*

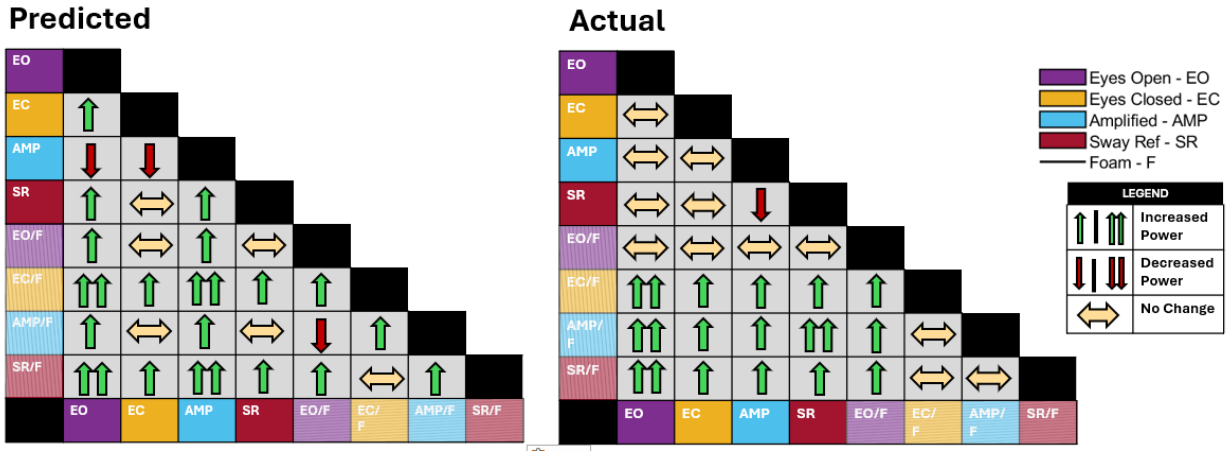

Figure 22: *This figure displays the FSCF-predicted responses (left) and the actual results (right) for the medium frequency band (0.5-1Hz) for AP COP. To interpret this figure, the condition on the y-axis is compared to the subsequent condition on the x-axis. The legends indicate both the condition and the direction of change. Hatched boxes indicate foam surface conditions. A single arrow indicates a predicted increase or decrease, whereas a double arrow indicates a stronger predicted change supported by changes in more than one variable.*

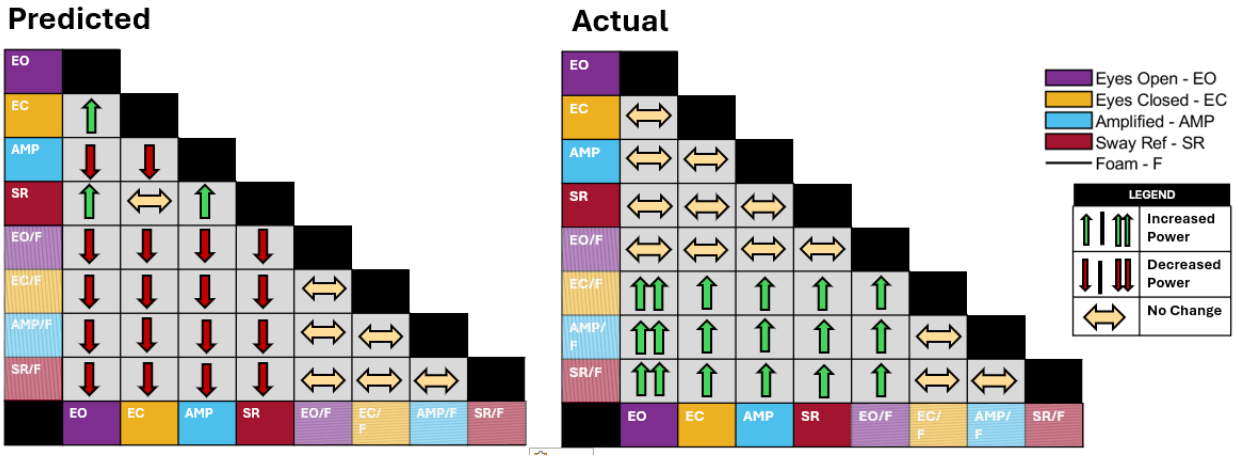

Figure 23: *This figure displays the FSCF-predicted responses (left) and the actual results (right) for the high frequency band (1-5Hz) for AP COP. To interpret this figure, the condition on the y-axis is compared to the subsequent condition on the x-axis. The legends indicate both the condition and the direction of change. Hatched boxes indicate foam surface conditions. A single arrow indicates a predicted increase or decrease, whereas a double arrow indicates a stronger predicted change supported by changes in more than one variable.*

Appendix B: AP COM FSCF Predictions vs Actual Results per condition

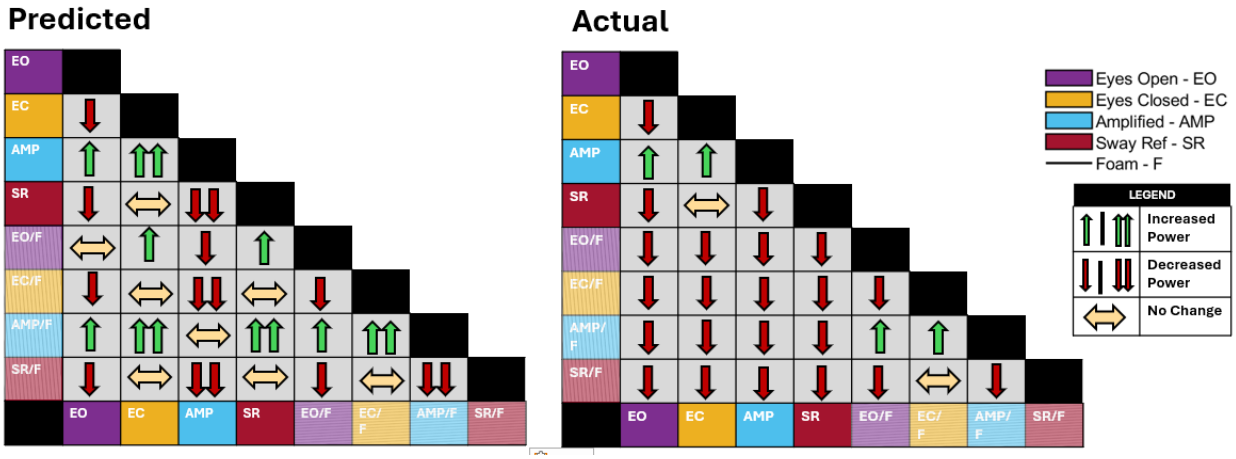

Figure 24: *This figure displays the FSCF-predicted responses (left) and the actual results (right) for the ultra-low frequency band (0-0.1Hz) for AP COM. To interpret this figure, the condition on the y-axis is compared to the subsequent condition on the x-axis. The legends indicate both the condition and the direction of change. Hatched boxes indicate foam surface conditions. A single arrow indicates a predicted increase or decrease, whereas a double arrow indicates a stronger predicted change supported by changes in more than one variable.*

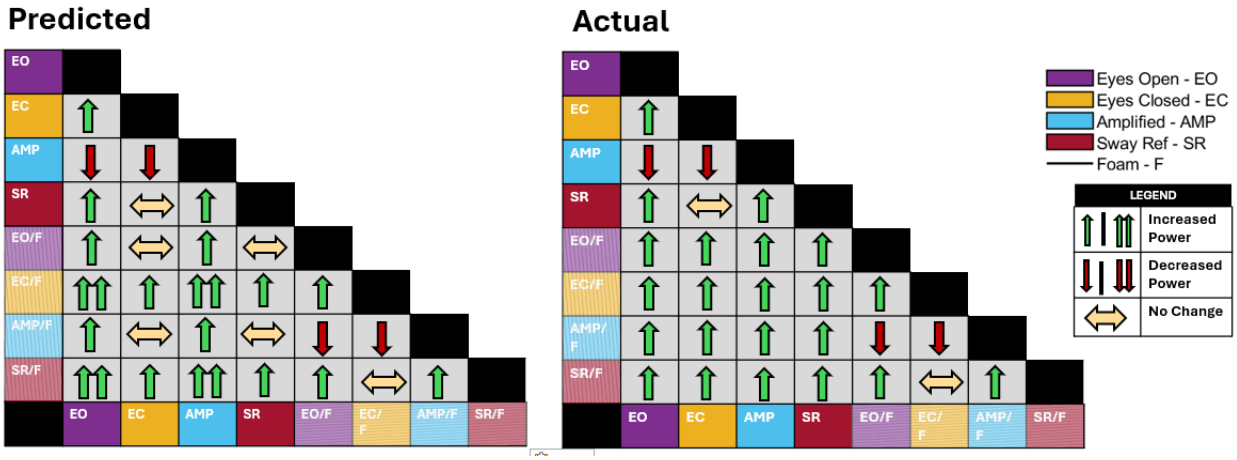

Figure 25: *This figure displays the FSCF-predicted responses (left) and the actual results (right) for the low frequency band (0.1-0.5Hz) for AP COM. To interpret this figure, the condition on the y-axis is compared to the subsequent condition on the x-axis. The legends indicate both the condition and the direction of change. Hatched boxes indicate foam surface conditions. A single arrow indicates a predicted increase or decrease, whereas a double arrow indicates a stronger predicted change supported by changes in more than one variable.*

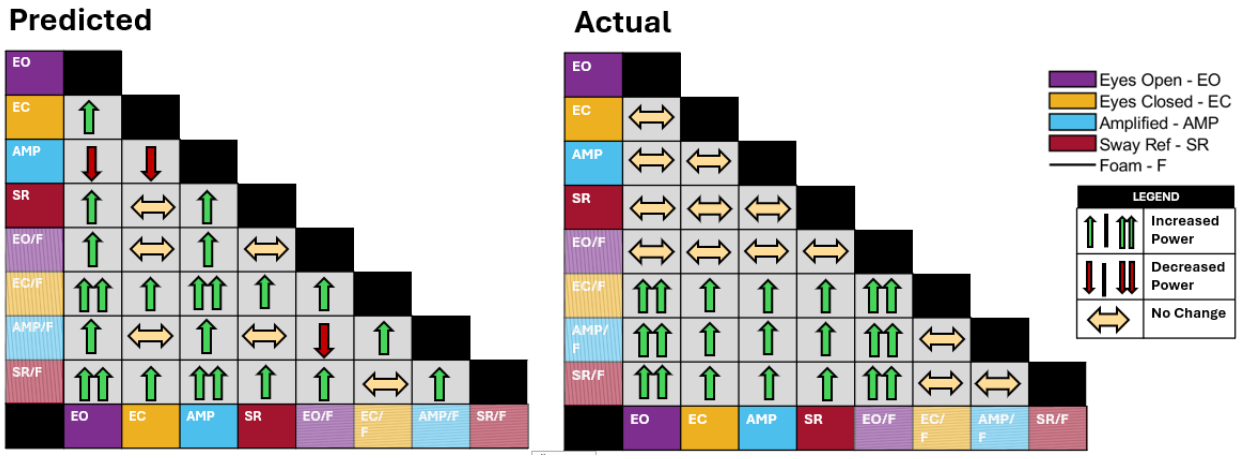

Figure 26: *This figure displays the FSCF-predicted responses (left) and the actual results (right) for the medium frequency band (0.5-1Hz) for AP COM. To interpret this figure, the condition on the y-axis is compared to the subsequent condition on the x-axis. The legends indicate both the condition and the direction of change. Hatched boxes indicate foam surface conditions. A single arrow indicates a predicted increase or decrease, whereas a double arrow indicates a stronger predicted change supported by changes in more than one variable.*

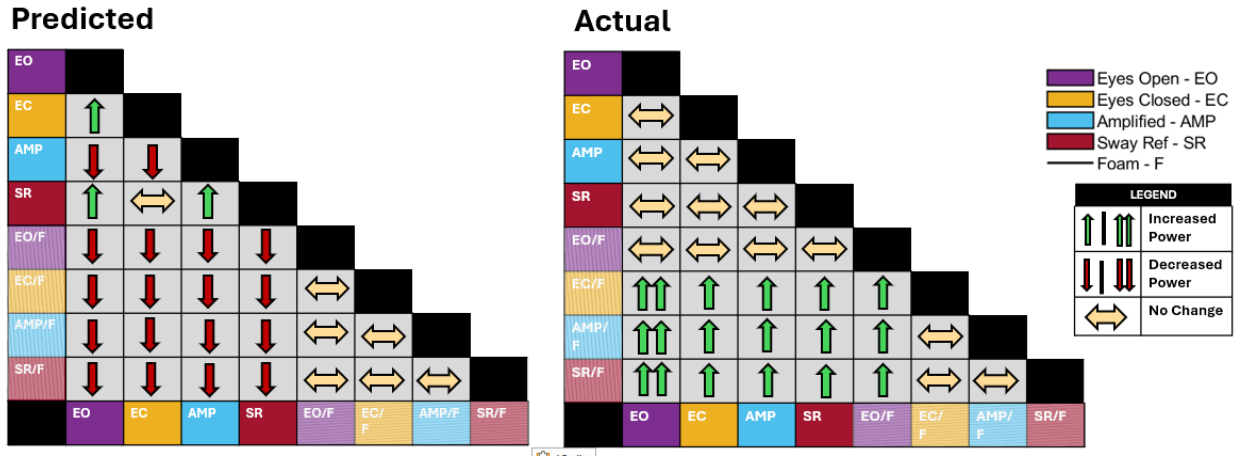

Figure 27: *This figure displays the FSCF-predicted responses (left) and the actual results (right) for the medium frequency band (0.5-1Hz) for AP COM. To interpret this figure, the condition on the y-axis is compared to the subsequent condition on the x-axis. The legends indicate both the condition and the direction of change. Hatched boxes indicate foam surface conditions. A single arrow indicates a predicted increase or decrease, whereas a double arrow indicates a stronger predicted change supported by changes in more than one variable.*

Appendix C: Low & High Frequency Control Figures ~ AP COP

Appendix C displays the relative frequency contribution of the AP COP for the low and high frequency control framework. The results of this analysis displayed a context-dependent relationship between the sensory conditions; however, changes between the sensory conditions can be described by changes to low and high frequency domain neural mechanisms. For example, in the low frequency domain, a significant interaction effect was identified ($F(1,31)=5.608$, $p=0.001$, $\eta^2=0.153$) and post-hoc tests confirmed significant differences between the visual conditions on the firm surface, visual conditions on the firm surface, and between form and foam conditions with a matched visual condition. Specifically, EO and SR visual conditions on the firm surface had a greater low frequency domain composition compared to EC and AMP visual conditions. The relationship between visual conditions on the firm surface was not identified using the frequency bands of the FSCF. On the foam surface, EO displayed a greater low frequency domain composition compared to EC, AMP, and SR visual conditions. Further, EC, AMP, and SR visual conditions on foam had a decreased low frequency domain composition compared to the matched visual condition on the firm surface. Figure 27 displays the results low frequency domain composition for the AP COP.

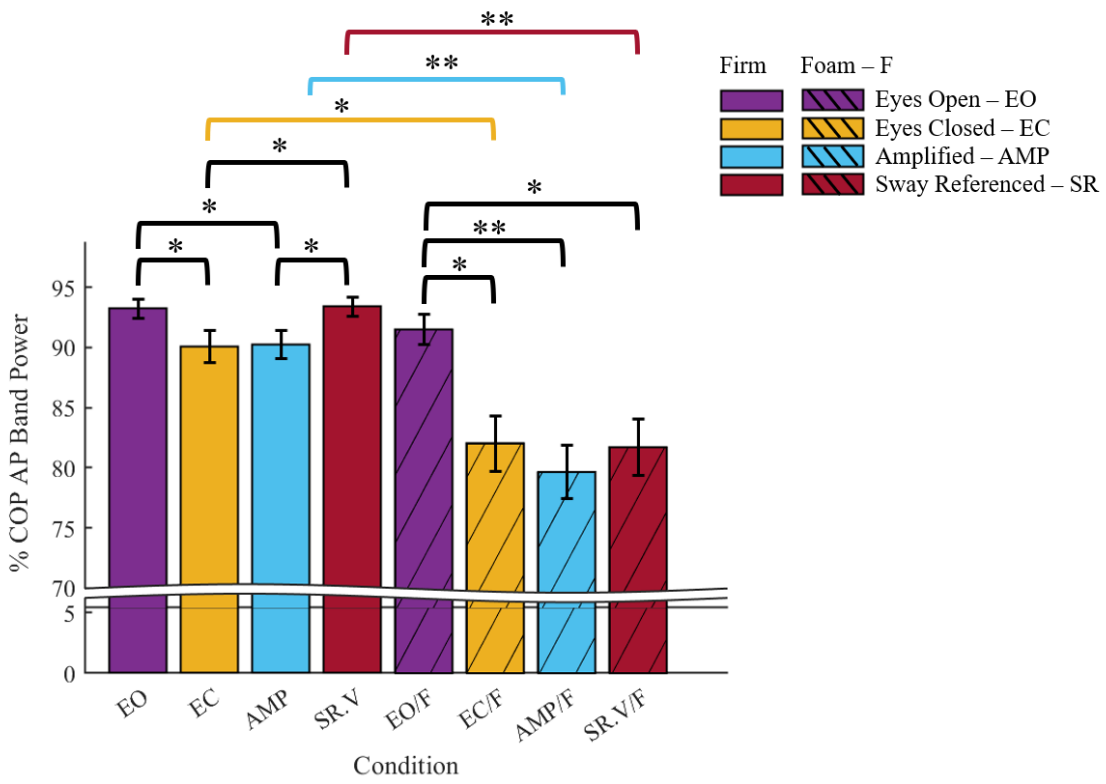

Figure 28: *Relative frequency composition of the AP COP for the low frequency domain (0-0.5Hz). Solid bars are firm surface conditions. Hatched bars are foam surface conditions. Colours represent visual conditions as indicated in the legend. Standard error bars are displayed. Significance is indicated between sensory conditions. (*p<0.005, **p<0.001).*

The results of the high frequency domain for AP COP displayed similar results to the medium and high frequency bands displayed in the thesis. A significant interaction effect was identified for the high frequency domain ($F(1,31)=5.552$, $p=0.002$, $\eta^2=0.152$). Post-hoc tests confirmed significant differences between the visual conditions on the firm surface, visual conditions on the firm surface, and between form and foam conditions with a matched visual condition. Specifically, the AMP visual condition had a greater high frequency domain composition compared to the SR visual conditions on the firm surface. On the foam surface, EO displayed a lower high frequency domain composition compared to EC, AMP, and SR visual conditions. Further, EC, AMP, and SR visual conditions on foam had an increased high frequency domain composition compared to the matched visual condition on the firm surface. Figure 28 displays the high frequency domain composition for the AP COP.

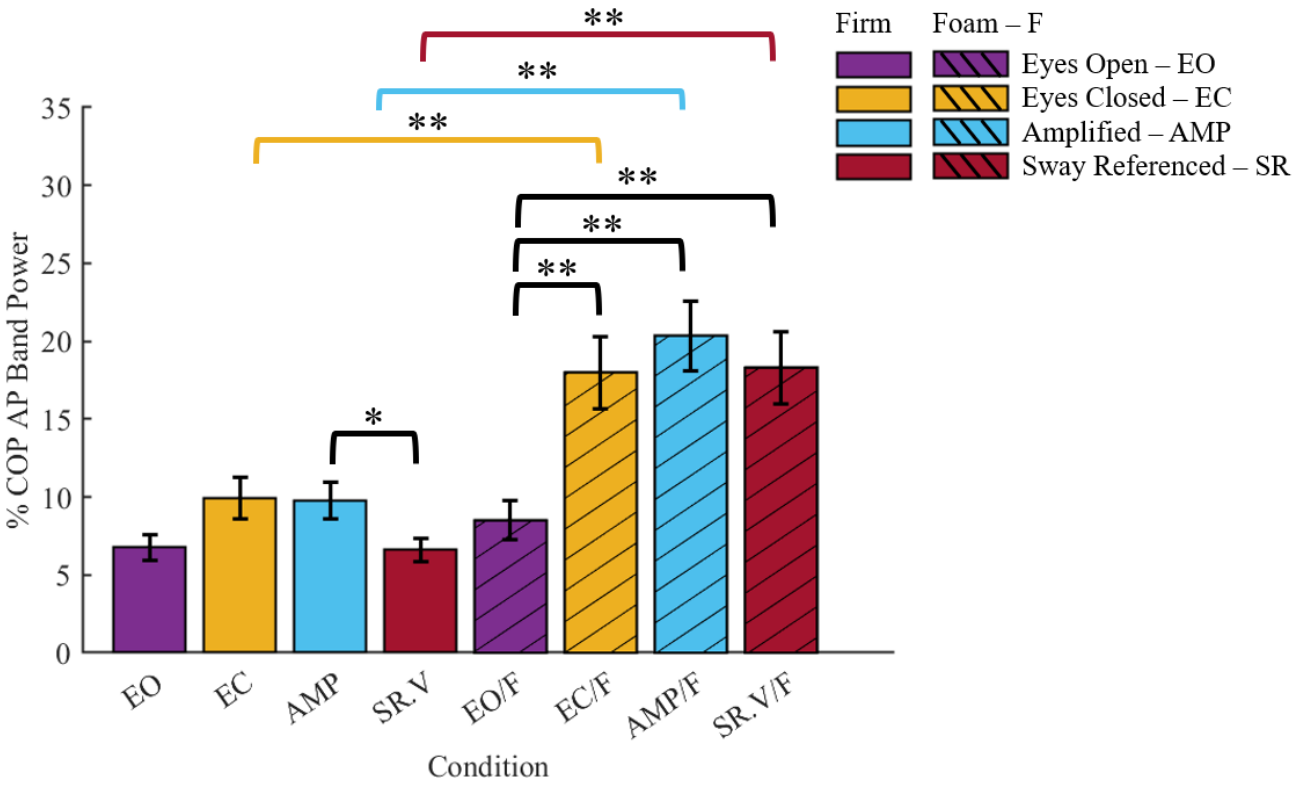

Figure 29: *Relative frequency composition of the AP COP for the high frequency domain (0.5-5Hz). Solid bars are firm surface conditions. Hatched bars are foam surface conditions. Colours represent visual conditions as indicated in the legend. Standard error bars are displayed. Significance is indicated between sensory conditions. (*p<0.005, **p<0.001).*